NAVAL POSTGRADUATE SCHOOL
MONTEREY, CALIFORNIA

THESIS

A SIMULATION OF PLASMA MOTION IN THE POLAR IONOSPHERE

by

David W. Deist

September, 1994

Thesis Advisor: D. D. Cleary

Approved for public release; distribution is unlimited.

REPORT DOCUMENTATION PAGE

Form Approved OMB No. 0704-0188

1. AGENCY USE ONLY *(Leave blank)*	2. REPORT DATE September, 1994	3. REPORT TYPE AND DATES COVERED Master's Thesis

4. TITLE AND SUBTITLE A SIMULATION OF PLASMA MOTION IN THE POLAR IONOSPHERE (u)	5. FUNDING NUMBERS
6. AUTHOR(S) Deist, David W	
7. PERFORMING ORGANIZATION NAME(S) AND ADDRESS(ES) Naval Postgraduate School Monterey CA 93943-5000	8. PERFORMING ORGANIZATION REPORT NUMBER
9. SPONSORING MONITORING AGENCY NAME(S) AND ADDRESS(ES)	10. SPONSORING MONITORING AGENCY REPORT NUMBER

11. SUPPLEMENTARY NOTES The views expressed in this thesis are those of the author and do not reflect the official policy or position of the Department of Defense or the U. S. Government

12a. DISTRIBUTION AVAILABILITY STATEMENT Approved for public release; distribution is unlimited	12b. DISTRIBUTION CODE A

13. ABSTRACT *(maximum 200 words)*

A model of plasma motion in the polar ionosphere is presented. Plasma motion due to polar convection and corotation above 50° N is modeled. The universal time (UT)-dependent corotation electric field (in the geomagnetic frame) is added to a polar convection electric field that is UT-dependent in the geographic frame and the total is displayed in both reference frames. To simulate actual magnetic conditions, varying polar convection patterns may be used by the model we have developed. Trajectories of single plasma parcels and regions of plasma are calculated. The calculated trajectories are displayed in the geographic and magnetic inertial reference frames. The model developed is applied to the study of a region of electron depletion near the pole, a polar hole. Changes in the size and location of the polar hole are explained in terms of a changing convection pattern. The results of this thesis are being used by the Johns Hopkins University Applied Physics Laboratory to further study ionospheric plasma motion.

14. SUBJECT TERMS Ionosphere, Electron Density, Plasma Motion, Polar Hole	15. NUMBER OF PAGES 60
	16. PRICE CODE

17. SECURITY CLASSIFICATION OF REPORT	18. SECURITY CLASSIFICATION OF THIS PAGE	19. SECURITY CLASSIFICATION OF ABSTRACT	20. LIMITATION OF ABSTRACT
Unclassified	Unclassified	Unclassified	UL

Approved for public release; distribution is unlimited.

A SIMULATION OF PLASMA MOTION IN THE POLAR IONOSPHERE

by

David W. Deist
Captain, United States Marine Corps
B.S., United States Naval Academy, 1985

Submitted in partial fulfillment
of the requirements for the degree of

MASTER OF SCIENCE IN ASTRONAUTICAL ENGINEERING

from the

NAVAL POSTGRADUATE SCHOOL
September, 1994

Author: _____
David W. Deist

Approved by: _____
David D. Cleary, Thesis Advisor

_____
Oscar Biblarz, Second Reader

_____
Daniel J. Collins, Chairman
Department of Aeronautics and Astronautics

ABSTRACT

A model of plasma motion in the polar ionosphere is presented. Plasma motion due to polar convection and corotation above 50° N is modeled. The universal time (UT)-dependent corotation electric field (in the geomagnetic frame) is added to a polar convection electric field that is UT-dependent in the geographic frame and the total is displayed in both reference frames. To simulate actual magnetic conditions, varying polar convection patterns may be used by the model we have developed. Trajectories of single plasma parcels and regions of plasma are calculated. The calculated trajectories are displayed in the geographic and magnetic inertial reference frames. The model developed is applied to the study of a region of electron depletion near the pole, a polar hole. Changes in the size and location of the polar hole are explained in terms of a changing convection pattern. The results of this thesis are being used by the Johns Hopkins University Applied Physics Laboratory to further study ionospheric plasma motion.

TABLE OF CONTENTS

ACKNOWLEDGMENT

I would like to thank Dr. Geoff Crowley for his support, knowledge, and patience. The Space Physics Department at the Johns Hopkins University Applied Physics Laboratory (JHU/APL) has provided an exceptional level of support that made my work with them a truly enjoyable learning experience. I could not have done this thesis without the computer expertise of Joe Blau at NPS and Dr. Bill Bristow at JHU/APL. I am indebted to Dr. David Cleary for his support, particularly during the writing and presentation of this thesis. Finally, I would like to thank my lovely wife, Vicki, and my family. Without their love and support, I could not have completed this thesis and my studies here at the Naval Postgraduate School.

I. INTRODUCTION

In a memorandum from the Joint Chiefs of Staff (1986), military requirements for environmental satellites operated by elements of the Department of Defense were prioritized. Among the 43 environmental parameters listed, ionosphere electron density ranked five, and ionospheric scintillation (change in electron density) ranked 31. The services broke their mission support requirements down into 12 areas ranging from command, control, communications, and intelligence (C^3I) to logistics. The Navy and Marine Corps listed electron density and ionospheric scintillation as applying, either directly or indirectly, to every mission support area. Ionospheric scintillation and electron densities influence high-latitude radars, and long-distance high frequency (HF) and transionospheric satellite communications.

Among the factors contributing to ionospheric scintillation and electron density fluctuations are solar enhancement, chemical recombination, and ionospheric plasma convection. Solar enhancement and chemical recombination are discussed briefly in Chapter two. Ionospheric plasma convection is the focus of this thesis. It can be thought of as existing in three distinct regions: the equatorial region, mid-latitudes ($\leq 50°$ latitude), and high latitudes ($\geq 50°$ latitude). The most dynamic and least understood is the high latitude region. Near the poles, areas of enhanced electron density (patches) and depleted electron density (holes) move quickly. As they move, communications windows are opened and closed. In an effort to understand how these holes and patches move, this thesis develops a computer model of ionospheric convection that can be used to simulate plasma motion above 50° latitude.

Theoretical studies are often expressed in a fixed magnetic reference frame. However, data obtained either from satellites or ground based instruments are generally expressed in a geographic reference frame. Comparison of theoretical and physical studies is difficult because the geographic and magnetic reference frames are in constant motion both in relation to each other and to the sun. To allow for practical comparison of theory and physical observations, we developed a tool for studying ionospheric plasma

motion in both reference frames. The plasma motion and the contributing ionospheric convection patterns can be displayed quickly and easily.

Computer algorithms were developed to calculate the trajectory of either a single parcel of plasma or a region of plasma and display the trajectory in both reference frames. The algorithms were developed using the Interactive Data Language (IDL) on a UNIX based computer. Algorithms written in Fortran and C previously developed at the Johns Hopkins University Applied Physics Lab (JHU/APL) are also used where convenient. Although the motivation for this thesis is based on the motion of a polar hole, it also has application in any study involving plasma motion at high latitudes.

In a theoretical study, Brinton et al. (1978) first described a polar hole, but it was not until recently that Crowley et al. (1993) performed the first detailed study of an actual polar hole. They presented the morphology of a polar hole based on data from the Geospace Environment Program (GEM) Pilot Program of 16 January 1990. The GEM Pilot Program involved the DMSP F8 and F9 satellites, a digital ionosonde, and a 250 MHz scintillation receiver. Figure 1 depicts the electron concentration measurements from the DMSP F8 satellite for 0136-0152 UT on 16 January 1990. The electron concentrations can be seen to vary by an order of magnitude on the edge of the polar hole. Figure 2 depicts the scintillation index from the 250 MHz receiving system at Thule, Greenland. Scintillation indexes as low as 0 dB were observed in the polar hole. Clearly, the polar hole plays an important role for any area of mission support affected by ionosphere electron concentration and scintillation. This thesis explains changes in location and size of a particular polar hole using the model developed. The results of this thesis tie in with the work by Crowley and his co-workers at Johns Hopkins University Applied Physics Lab (JHU/APL) in the study of the dynamic motion of the polar hole.

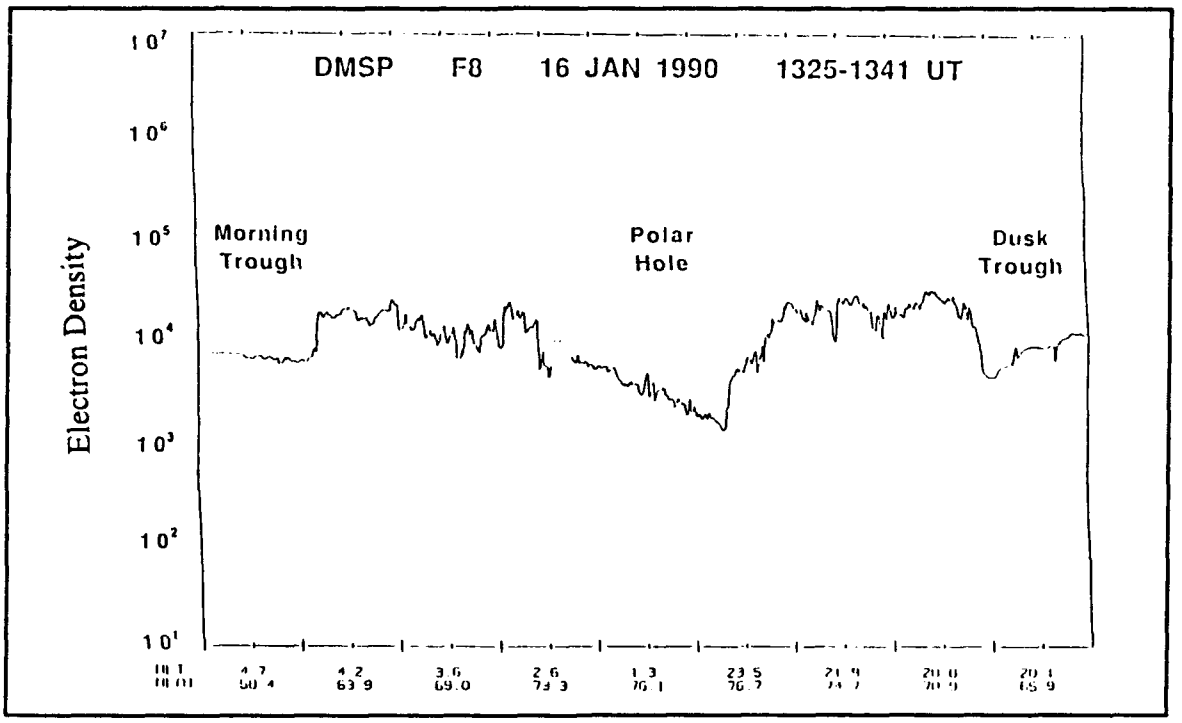

Figure 1. Depiction of electron concentration measurements from the DMSP F8 satellite for 0136-0152 UT, 16 January 1990

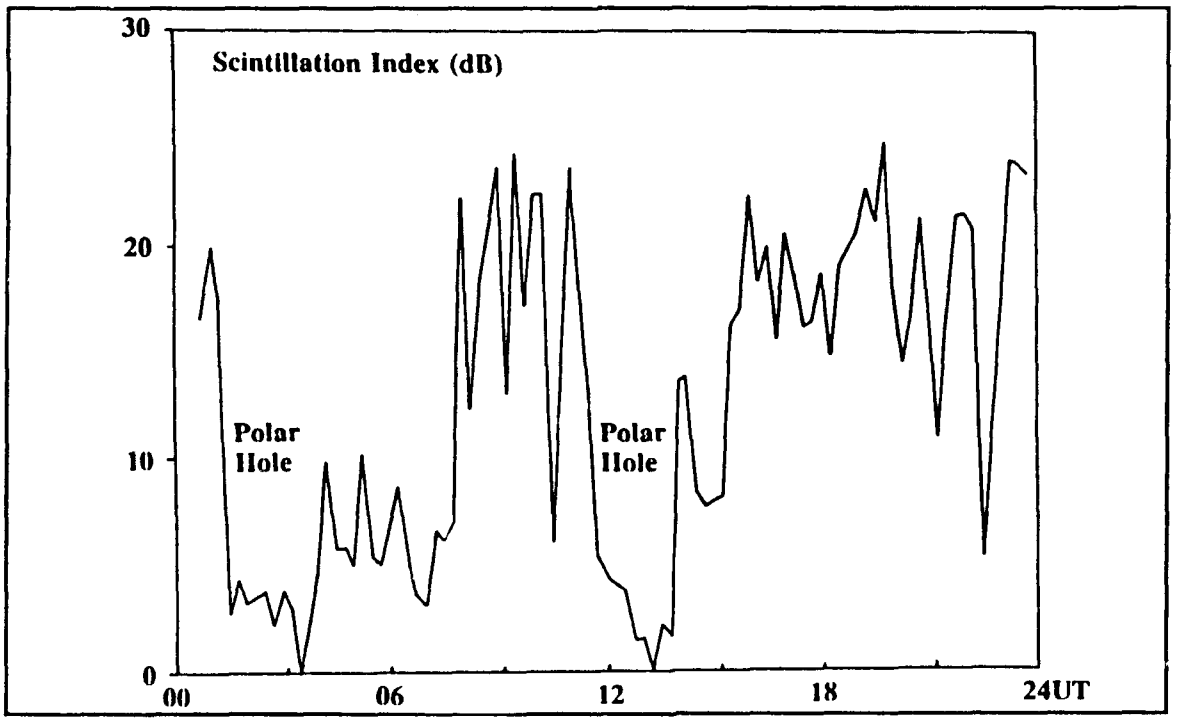

Figure 2. Scintillation index from 250 MHz receiver at Thule, Greenland for 16 January 1990

II. BACKGROUND

A. GENERAL

The goal of this thesis is to provide a tool for studying the motion of plasma, polar holes and patches. The electron production and loss mechanisms that cause the holes and patches are not considered. They are, however, important in understanding the significance of the plasma trajectories calculated and will be mentioned here briefly.

Free electrons are produced by 1) the ionization of neutral gases by solar ultraviolet (UV) and x-radiations, and 2) by energetic electrons that follow the geomagnetic field lines from the magnetosphere and collide with neutrals. Free electrons are lost by chemical recombination and diffusion. If a region of plasma stagnates in an area where the loss rate is greater than the production rate, the electron density will decrease. And if a region of plasma moves into an area of greater production, the electron density will increase (Kelley, 1989). It is important to note that the changes in size and shape of holes and patches in our model are the result of plasma motion and no production or loss mechanisms are considered.

Two sources of plasma motion will be considered. One, polar convection, is caused by interaction of the earth's magnetic field with the solar wind (Kelley, 1989). The other is corotation with the earth (Davis, 1947, 1948) (Hones et al., 1965). It will be shown that plasma motion is along lines of equipotential, therefore, the paths of plasma convection may be displayed as patterns of equipotentials (Kelley, 1989). This chapter will present these equipotential patterns, explain their sources, and describe the modelling techniques used to obtain them.

B. POLAR ELECTRIC FIELDS

Polar convection is caused by the polar electric fields. Both are central to any discussion of polar plasma flow, therefore a thorough understanding of the polar electric fields and resulting convection is necessary. Plasma convection at high latitudes can be characterized typically by the two-cell equipotential pattern shown in Figure 3. In

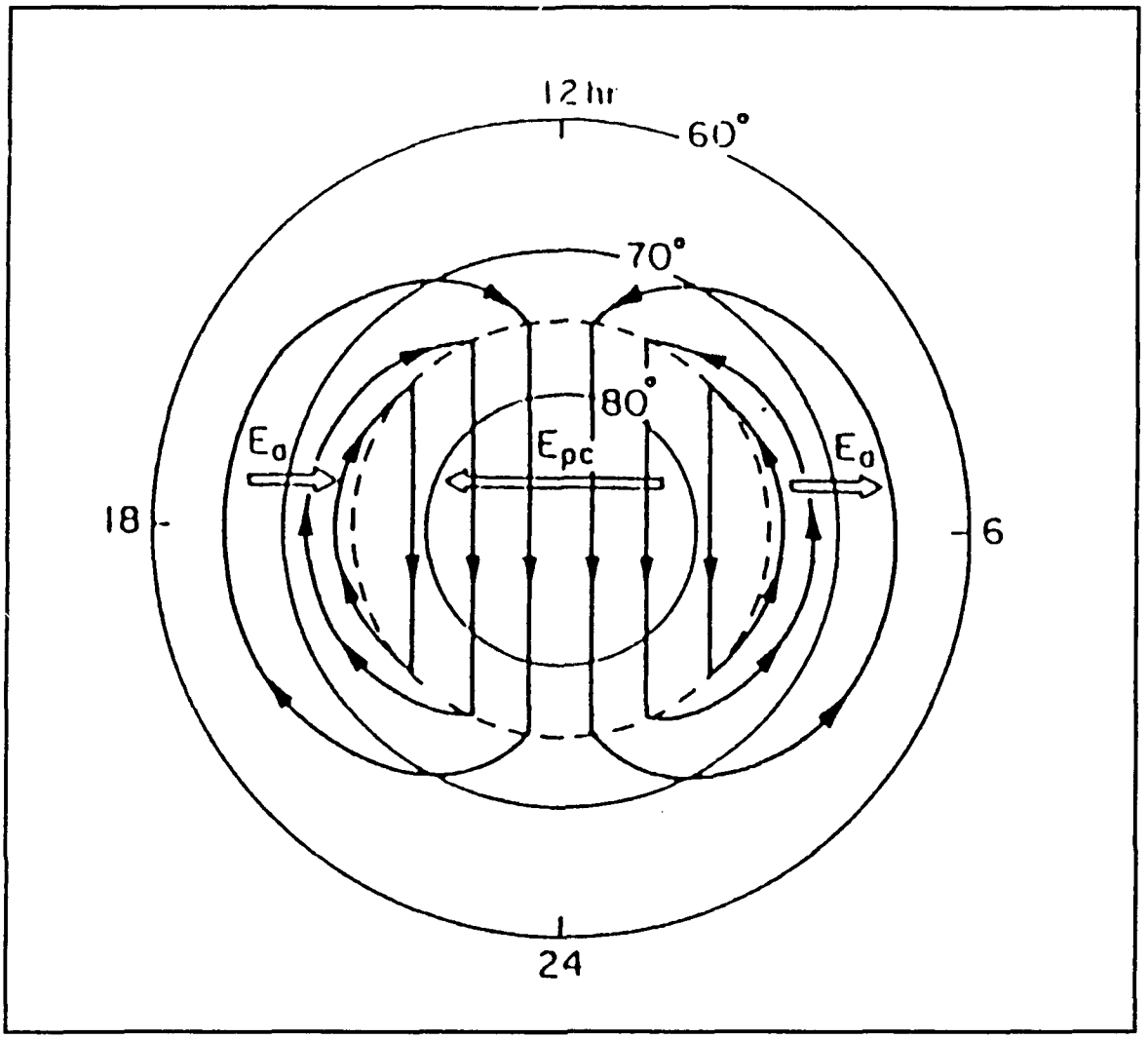

Figure 3. Representation of ionospheric electric fields in the northern hemisphere polar cap, as well as plasma flow due to those fields. From Kelley (1989).

addition to the plasma flow patterns shown, there are three electric fields, one is labeled E_{pc} and two are labeled E_a. First we will discuss these three electric fields, then we will explain the relationship between the electric fields and the plasma flow. Finally, we will discuss the two-cell pattern of Figure 3 in detail (From Kelley, 1989).

All three electric fields have their origin in the magnetosphere. The magnetosphere, shown in Figure 4, is the result of the interaction between the earth's magnetic field and the solar wind. Magnetic field lines in the magnetosphere can be classified as either open or closed. Open field lines have one foot on the earth and

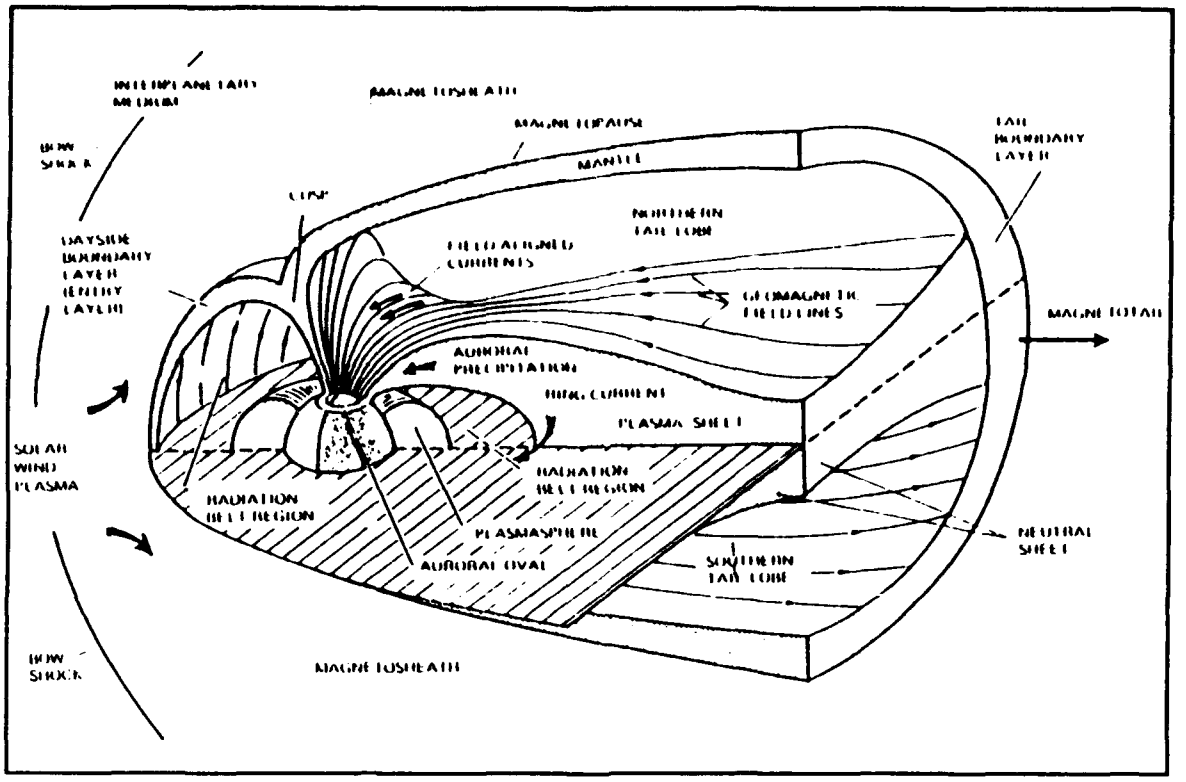

Figure 4. Schematic representation of the magnetosphere. From Kelley (1989)

another that extends into the magnetosheath and interacts with the solar wind. Closed field lines have both feet on the earth. We will show that the electric field, E_{pc} is generated by the open field lines and the two E_a fields are generated by the closed field lines.

To understand the relationship between the field lines, plasma velocities, and electric fields, the following equations are needed. The plasma drift velocity, **V**, is given by

$$\mathbf{V} = \frac{\mathbf{E} \times \mathbf{B}}{\mathbf{B}^2} \qquad (2.1)$$

where **E** is the electric field and **B** is the magnetic field. At times it will be necessary to find the electric field given the velocity and magnetic field. Manipulating Equation (2.1) and solving for **E** yields

$$\mathbf{E} = -\mathbf{V} \times \mathbf{B} \qquad (2.2)$$

Figure 5 depicts the open field lines interacting with the solar wind. At the top of the figure, the solar wind is traveling at a velocity, V_{sw}, away from the sun. The magnetic field lines are pointing toward the earth. From Equation (2.2), the electric field will point from dawn to dusk. Since electrons can flow freely along magnetic field lines, the field lines are lines of constant potential. Thus, any potential difference at one end of a pair of magnetic field lines will be present at the other end. Referring back to Figure 5, the magnetic field line on the left will have a higher potential than the line on the right.

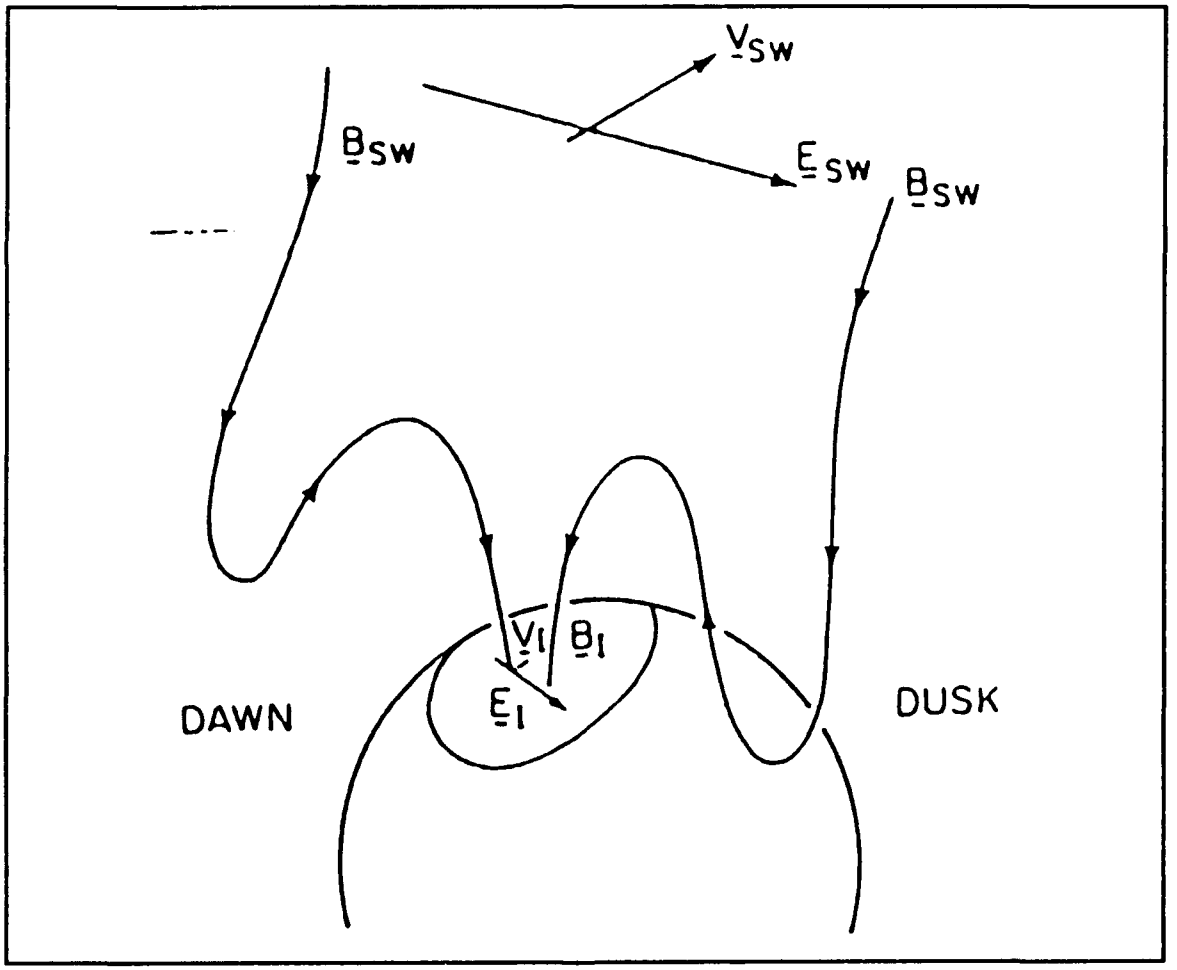

Figure 5. Schematic representation of the magnetic connection between the magnetosphere and the ionosphere. From Kelley (1989).

So at the ionosphere there must be an electric field pointing from dawn to dusk. This electric field is labeled E_I in Figure 5 and E_{ps} in Figure 3

A similar argument is used to explain how closed field lines are responsible for the two electric fields labeled E_s in Figure 3. The closed field lines extending into the boundary layer and plasma sheet are distorted from a dipole shape into a magnetic tail extending away from the sun. This magnetic geometry creates a tension that exerts a force on the plasma. This force is combined with potential differences and pressure gradients across the magnetopause to cause a motion of the plasma across the closed field lines toward the sun. The magnetic field lines in the magnetotail are perpendicular to the sunward velocity as shown in Figure 6. Just as an electric field was produced by the solar wind moving past the open field lines, a dawn-to-dusk electric field is produced in the magnetotail by the sunward flow past the closed field lines. Again, the field lines are equipotentials. Referring to the two field lines on the right or dusk side, the outermost

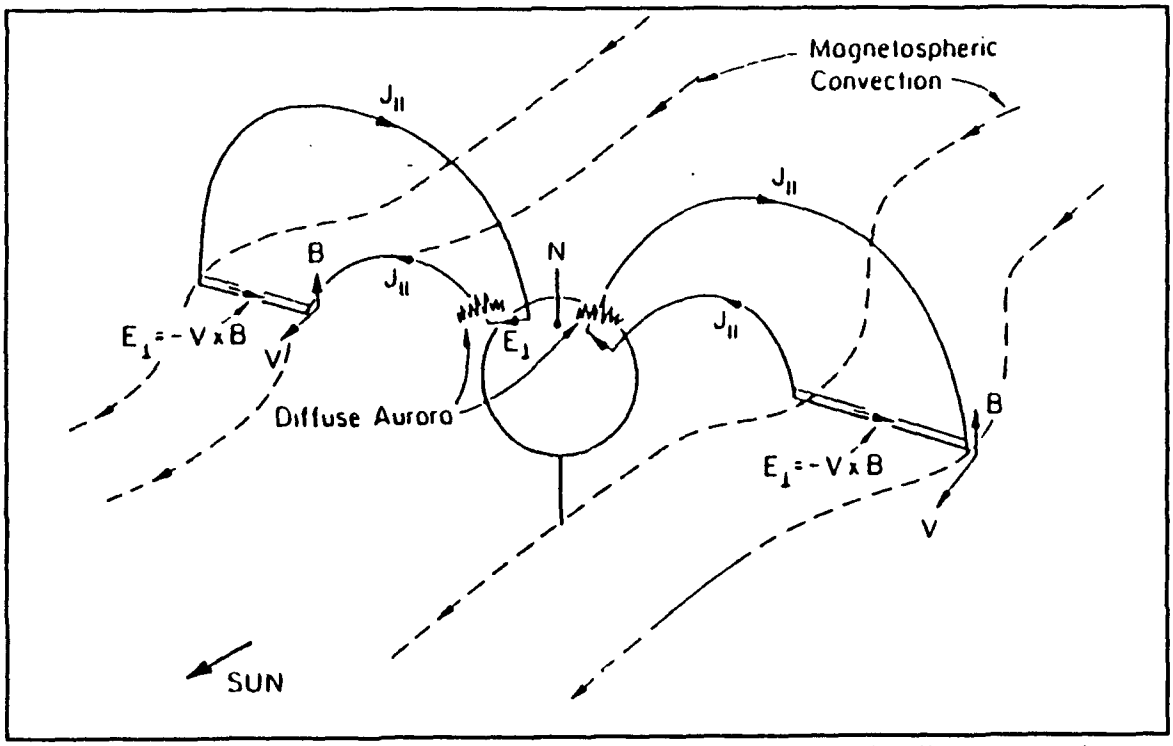

Figure 6. Three-dimensional view of the closed magnetospheric filed lines mapped to the ionosphere. From Kelley (1989)

line is at a lower potential than the inner line. In the ionosphere, this potential difference produces a dusk-to-dawn electric field. In the same manner, a dusk-to-dawn electric field is produced on the dawn side. These are the electric fields labeled E_a in Figure 3.

This explains the origin of the electric fields shown in Figure 3. Using Equation (2.1) and assuming the magnetic field in Figure 3 is into the figure, we know that the plasma flow due to E_{pc} is away from the sun. Likewise, the flow due to E_a is toward the sun. Combining the two produces the two-cell pattern shown. This pattern will be referred to as the polar convection pattern.

Figure 3 is the simplest example of polar convection. It has a two-cell pattern with the cell on the right referred to as the dawn cell and the cell on the left referred to as the dusk cell. The dawn cell will have a positive potential and counter-clockwise motion. The dusk cell will have a negative potential and clockwise motion. The combination of the two produces anti-sunward flow over the pole and sunward flow at lower latitudes. The potential difference between the two cells is referred to as the polar cap potential drop and is used as a measure of strength for the polar convection.

The actual shape of the polar convection pattern is dependent on the orientation of the Interplanetary Magnetic Field (IMF). The coordinate system for the IMF has its center at the center of the earth. Positive x is pointed toward the sun. Positive z is pointed northward along the earth's spin axis. Positive y is determined by the right hand rule and points toward the dusk sector. Figure 7 depicts two polar convection patterns that occurred on 16 January 1990 under differing IMF conditions. Both the IMF B_y and B_z components were positive in Figure 7a and both were negative in 7b. The polar cap potential drop in Figure 7a is only 20 kV and most of the potential difference is located in the dusk cell (typical of a B_z positive condition). In Figure 7b the polar cap potential drop is 32 kV and most of the potential difference is in the dawn cell (typical of a B_z negative condition). The time scale for changes in the IMF at the poles varies from minutes to hours. The potential pattern responds to changes in the IMF within about five to ten minutes. Consequently, the potential patterns are extremely variable.

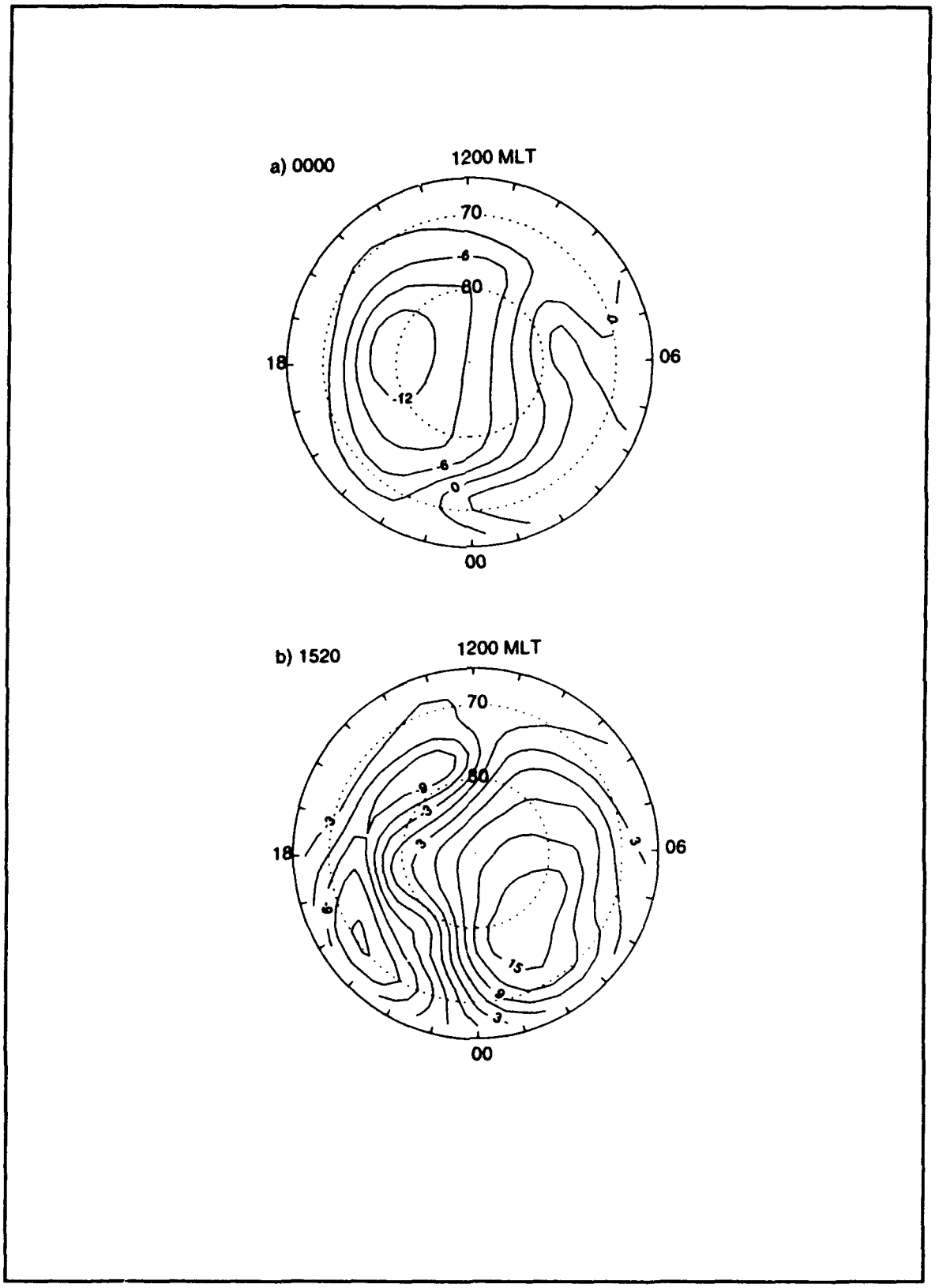

Figure 7. Polar convection equipotential patterns for 16 January 1990

Two techniques are used to model the polar potentials: 1) a model developed by Heelis et al. (1982) and 2) the Assimilative Mapping of Ionospheric Electrodynamics (AMIE) technique of Richmond et al. (1988). Only their applicability to this thesis will be mentioned below. For detailed descriptions of their development and capabilities, the reader is referred to the references.

1. Heelis Model

This model was developed by Heelis et al. (1982). Mathematical expressions were developed that eliminate discontinuities in the ion convection velocities. Its purpose is to reproduce the large-scale characteristics of high-latitude ionosphere convection. The output of the model is an equipotential pattern that represents potentials from magnetospheric source only, corotation is not included. The Heelis model can only generate two-cell patterns typical of southward B_z conditions. It is used in this thesis to generate varying convection patterns. The model developed here has the capability to change the Heelis model patterns at specified times, thus simulating changes in the IMF orientation and the subsequent motion of the plasma.

2. AMIE Model

To model the actual polar convection patterns for 16 January 1990, the Assimilative Mapping of Ionospheric Electrodynamics (AMIE) technique of Richmond et al. (1988) was used. The AMIE algorithms produce convection patterns based on electrodynamic data from various sources including electric fields from radar and satellites, electric currents from radars, and magnetic perturbations at the ground and at satellite heights. The algorithm makes use of statistical information containing averages and variances of the electrodynamic fields. It also quantifies the errors inherent in the mapped fields taking into account the distribution of available data, their errors, and the statistical errors of the fields.

The Heelis model lacks the ability to define the actual electric field at any one moment in time. In contrast, the AMIE technique tries to map the electric field at a given time over the entire polar region. The electric field is the direct calculation from a mapped equivalent current pattern derived from all available data sources. AMIE

potentials were obtained at ten minute intervals for the entire 24 hour period of 16 January 1990. A ten minute interval was chosen because the best time resolution of the available data was 10 minutes. The AMIE potentials can be used to calculate polar plasma trajectories for 16 January 1990. These calculated trajectories can be compared with the actual motion of the polar hole as described by Crowley et al. (1993). It should be noted that the polar cap potential drops found using the AMIE technique can be low due to averaging and differences between data and statistical information (Richmond et al., 1988). The accuracies of the polar cap potential drops do not affect the results of this thesis, but should be considered in further research conducted with the results.

C. COROTATION

The second source of plasma convection we consider is corotation. As the earth rotates, so does its magnetic field. Hones et al. (1965) showed, based on the work of Davis (1947,1948), that plasma surrounding a rotating, conducting, magnetized sphere will rotate with the sphere. Observations have shown that plasma at ionospheric heights does, in fact, tend to corotate with the earth. Viewed from the earth, the velocity and electric field due to corotation is zero. Viewed from a non-rotating frame, an inertial frame, there is a velocity (and hence electric field) present due to corotation. Whether the electric field causes the velocity or the velocity causes the electric field is academic. It is important that both exist and can be calculated. Equation (2.1) allows us to calculate a velocity resulting from a magnetic and electric field. Since we know the corotation velocity exists, there is an implied electric field. In fact, Hones et al. (1965) showed that the corotating electric field can be approximated by Equation (2.2). To better understand the relationship between the electric field and the velocity, we refer to Figure 8. Looking down over the north pole, we assume the magnetic field is into the figure at all points. For the velocity to be in a circular counter-clockwise motion, from Equation (2.2), the electric field must point toward the outside of the circle (south) at all points. Assuming a uniform magnetic field, lines of equipotential will form concentric circles around the spin axis, as represented by the dashed lines in Figure 8. In reality, the earth's magnetic field

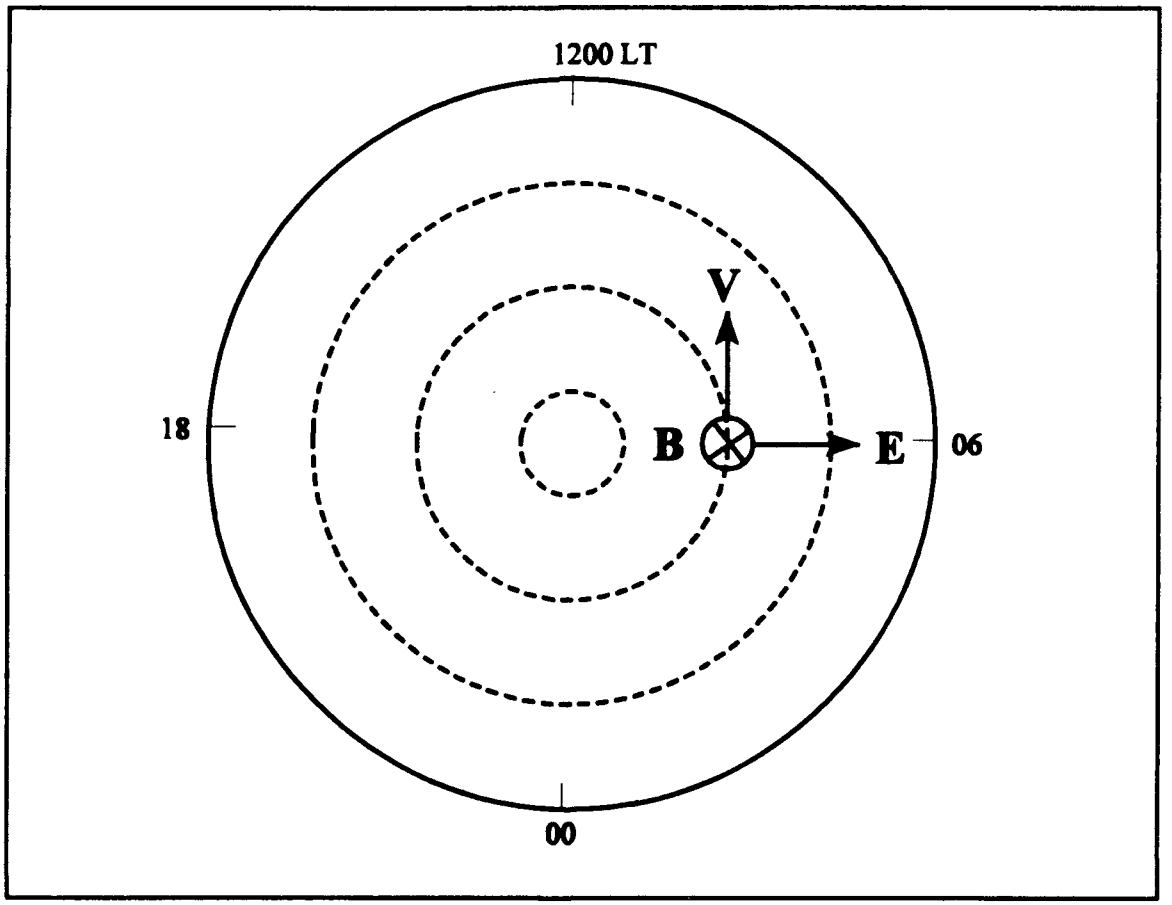

Figure 8. Schematic of the relationship between the corotating velocity and electric field.

is non-uniform and the magnetic pole is offset from the geographic pole. Consequently, the equipotential pattern for corotation is a series of concentric ellipses as in Figure 9.

D. PLASMA MOTION

Two sources of electric fields have been presented: polar convection and corotation. It was stated that plasma will flow along lines of equipotential for these fields. We will now show why. The electric field can be described by a potential ϕ using

$$\boldsymbol{E} = -\nabla\phi \tag{2.3}$$

Thus the electric field is perpendicular to lines of constant potential. The electric field is also perpendicular to the velocity found using Equation (2.1). Therefore, plasma flows along lines of constant potential and an equipotential pattern represents the plasma flow pattern (Kelley, 1989).

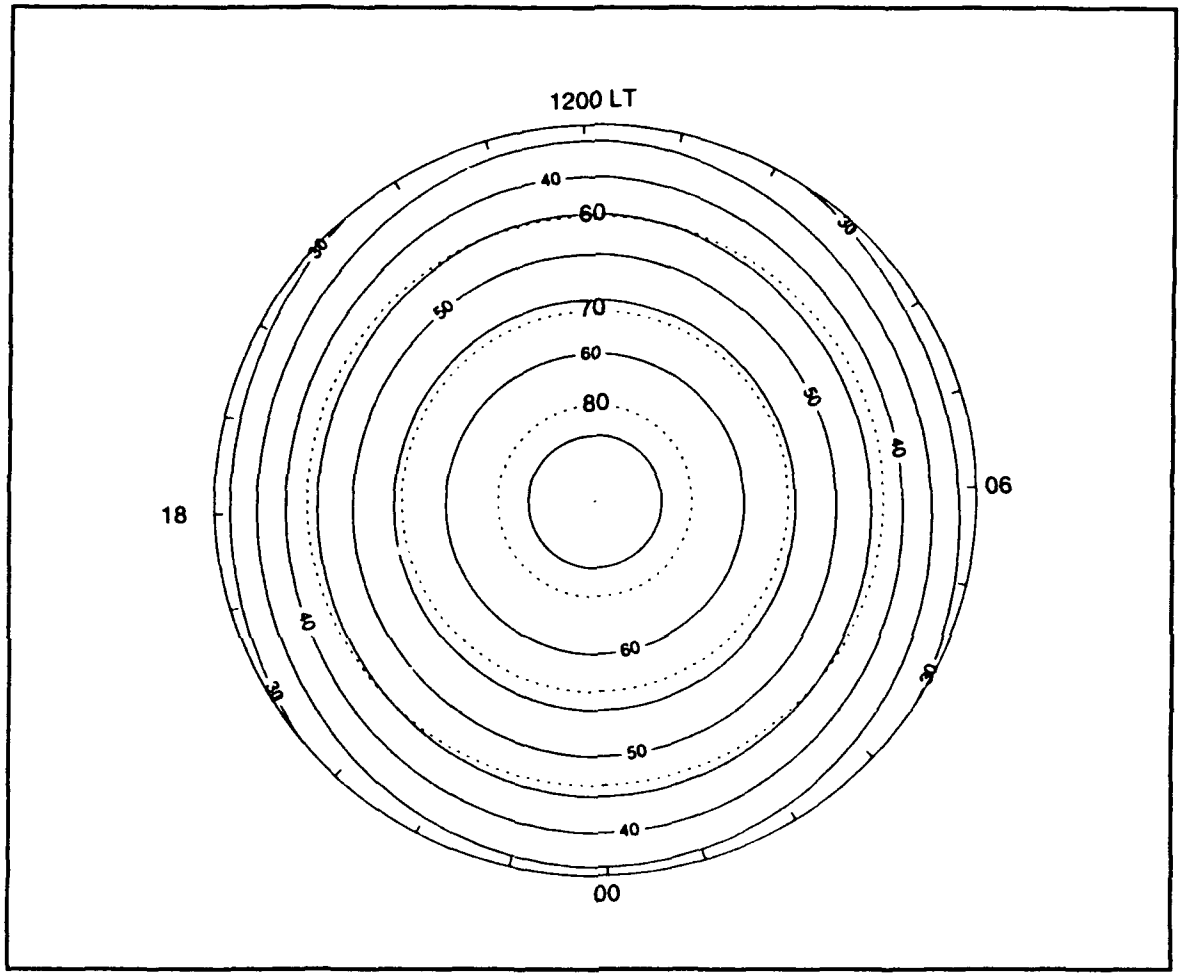

Figure 9. Depiction of the earth's corotation equipotential pattern in the geographic inertial reference frame.

III. COORDINATE SYSTEMS

In Chapter II, equipotential patterns from polar convection and corotation were established. Ultimately, the two convection sources will be combined and the total pattern will be displayed in both the geomagnetic and geographic reference frames. But, first, an explanation of the coordinate systems and reference frames is in order. Because the polar convection pattern has its origin in the magnetosphere, it is properly displayed in a magnetic inertial frame. The corotation pattern is properly displayed in a geographic inertial reference frame as discussed in Chapter II. The two reference frames and conversions between them will be discussed in this chapter. The patterns will then be combined in Chapter IV.

A. REFERENCE FRAMES

Positions in the magnetic inertial reference frame are expressed in geomagnetic latitude and magnetic local time (MLT). Figure 7 is displayed in the magnetic inertial reference frame. Magnetic local time is defined as the angle between the plane containing the earth-sun line and the magnetic axis of the earth and a line from the center of the earth to the position of interest. An angle of zero degrees corresponds to 1200 MLT. With the sun always assumed to be toward the top of the figure, 1200 MLT is also at the top and 2400 MLT at the bottom. The earth's eastward rotation will be in a counter-clockwise motion in this reference frame. Therefore, 0600 MLT, dawn, will be on the right and 1800 MLT, dusk, will be on the left.

Positions in the geographic reference frame are expressed in geographic latitude and local time (LT), as in Figure 9. Local time is defined as the angle between the plane containing the earth-sun line and geographic axis of the earth and the line from the center of the earth to the position of interest. Geographic longitude can be converted to LT using the following equation:

$$\mathrm{LT\,(degrees)} = \mathrm{geographic\ \ longitude} + \frac{\mathrm{UT} * 360}{24} \qquad (3.1)$$

where UT is universal time in hours. Just as 1200 MLT was at the top of the magnetic reference frame, 1200 LT will always be at the top of the geographic reference frame.

B. COORDINATE CONVERSIONS

To study the magnetic field at the polar region, a conversion was needed that would provide a smooth and well defined magnetic coordinate system at high latitudes. The PACE Geomagnetic Coordinate (PGM) system was designed by Baker and Wing (1989) to do exactly that. A series of FORTRAN routines were developed that provide a smooth conversion from geographic to geomagnetic coordinates for altitudes from 0 km to 600 km using an expansion of the geographic to geomagnetic relationship in spherical harmonics. Routines were also developed that do the inverse transformation. The coordinate system is produced by tracing magnetic field lines using the IGRF85 reference magnetic field model. One effect of tracing magnetic field lines to establish a coordinate system is that the spacing between lines of latitude will not be evenly spaced as lines of geographic latitude are.

MLT will typically be described in hours and can be given by :

$$\text{MLT (hrs)} = \phi / 15 + \text{const} + \text{UT} \tag{3.2}$$

where ϕ is the magnetic longitude of the point of interest, and the constant is dependent on the point of reference chosen. For the reference point of 0°N, 0°E geographic, the constant is -4.73 hours (-70.95 degrees). Although Equation (3.2) would have provided acceptable accuracy, Fortran routines developed by Baker and Wing (1989) were readily available to calculate magnetic local time accounting for the seasonal motion of the sun in declination and variations due to the eccentricity of the Earth's orbit and are used for our model.

IV. CONVECTION PATTERNS

The equipotential patterns are a convenient way to represent the plasma convection. This plasma convection depends on the combination of polar convection and corotation. In principle, the combined equipotential can be obtained by converting the polar convection potentials to geographic coordinates and adding corotation potentials (or vice versa). However, we have found it more convenient to add the electric fields. Therefore, when combining corotation and polar convection, the electric fields (potential differences) are added, not the individual potentials. Once the electric fields are combined, an equipotential pattern may be used to represent the plasma flow.

Key problems in obtaining the equipotential patterns are 1) where to set the potential to zero 2) the fact that integrating from the equator to the pole along meridians leads to multiple potential values at the pole and 3) integration in magnetic coordinates is different because magnetic lines of latitude are derived from mapping magnetic field lines, and are not evenly spaced. For this thesis we have solved the problems by the following: 1) the integration is done in the geographic reference frame, 2) an arbitrary value of 100 kV is assigned at the pole and the integration is done from the pole along lines of longitude to 30° N latitude, 3) an average potential value is found at 30° N latitude, and 4) the average is subtracted from each point, so that the potentials are all referenced to an average of zero at 30° N latitude.

A. POLAR CONVECTION IN THE GEOGRAPHIC REFERENCE FRAME

To display the polar convection pattern in the geographic reference frame, geographic positions desired for plotting are converted to magnetic coordinates, then potentials for each position are found using either the AMIE technique or the Heelis model.

Figure 10 depicts the polar convection pattern in the geographic reference frame at six hour intervals over 18 hours. The general relationship between the geographic and magnetic reference frames can be best understood by considering the dipole model of the geomagnetic field. For the dipole model, the geomagnetic north pole is assumed to be at

a geographic position of about 79°N and 71° W. At 0000 UT (Figure 10a), the prime meridian is located at 0000 LT, hence the geomagnetic pole and the center of the polar convection pattern is offset 11° in latitude and -70° in longitude or at approximately 1930 LT. Because the polar convection pattern is the result of interaction between the solar wind and IMF, the pattern will maintain its orientation in relation to the sun with anti-sunward flow over the magnetic pole and return flow at lower latitudes. At 0600 UT, Figure 10b, the prime meridian has moved six hours to 0600 LT, and the geomagnetic pole and center of the polar convection pattern have moved six hours to 0130 LT. Likewise, at 1200 UT, Figure 10c, the center of the polar convection pattern is offset toward 0730 LT. The orientation to the sun remains unchanged. This counter-clockwise motion in an inertial reference frame due the rotation of the earth is typically referred to as universal time (UT) motion.

In Figure 11, corotation is added to the polar convection patterns and they are displayed at six hour intervals over 18 hours just as in Figure 10. The effect of adding corotation is to enhance the counter-clockwise flow of the polar convection pattern and deplete the clockwise flow. This is best seen in Figure 11a where the resulting pattern is close to symmetric. The center of the polar convection pattern (anti-sunward flow) is offset by about 11° toward 1930 LT just as in Figure 10a. Over the 18 hour period, the center of the pattern moves in counter-clockwise motion as it did in Figure 10. The affects of this UT motion on plasma flow will be discussed in Chapter VI.

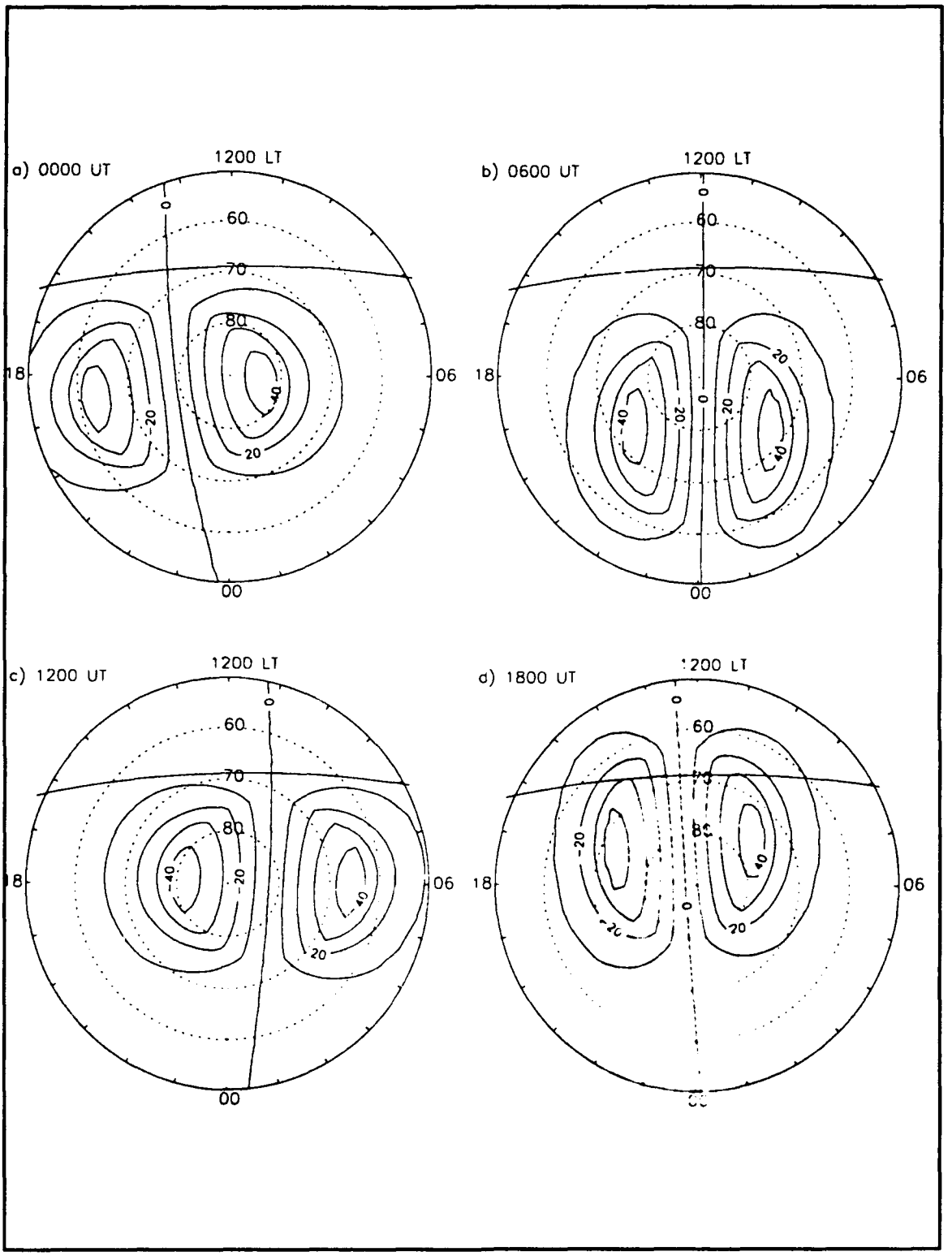

Figure 10. UT motion of the polar convection pattern in the geographic inertial frame. Potentials are labeled in kV. The solid line in the noon sector is the terminator at the surface.

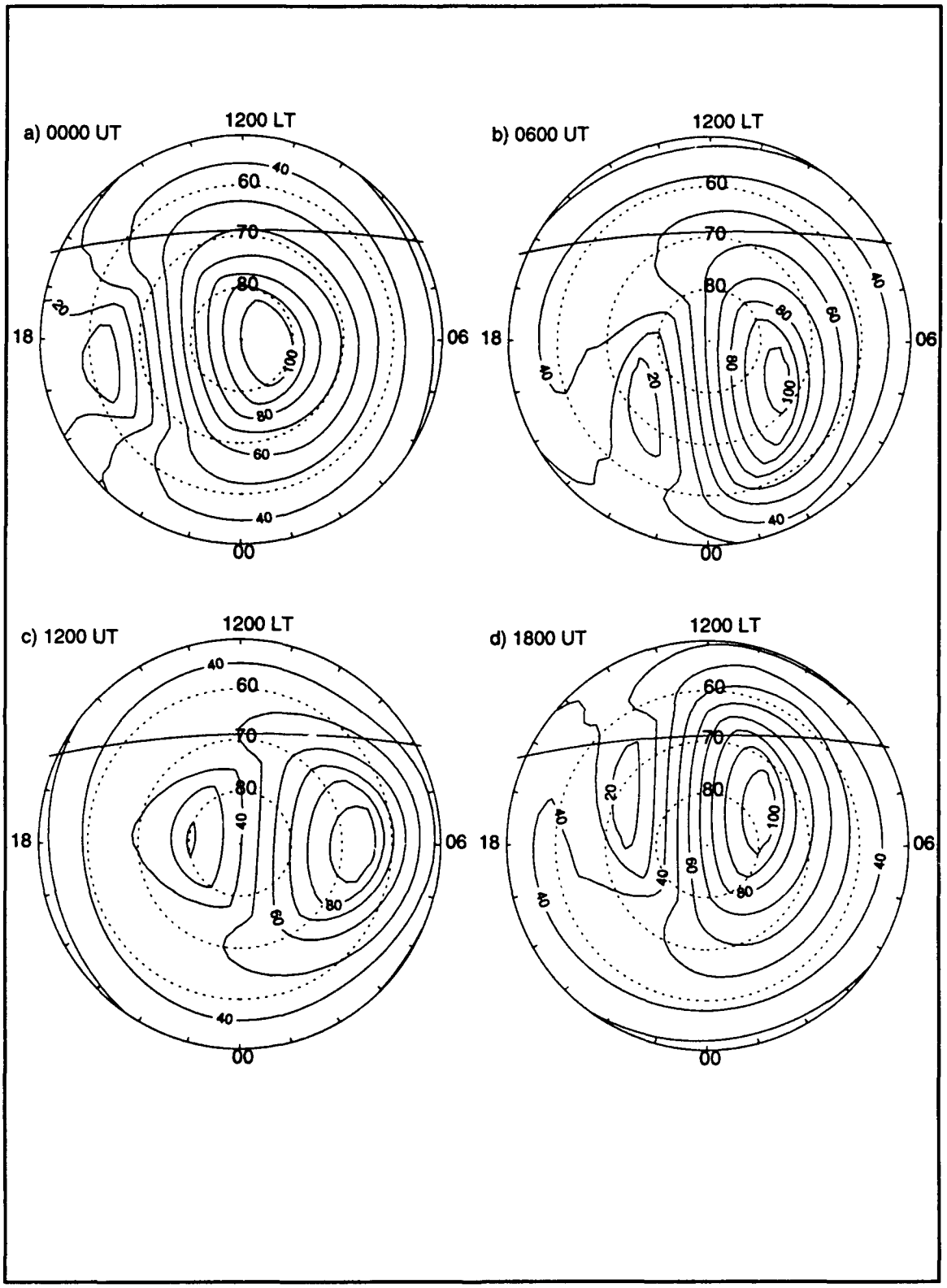

Figure 11. The total convection pattern in the geographic reference frame. Potentials are in kV. The solid line in the noon sector is the terminator on the ground.

B. COROTATION IN THE MAGNETIC REFERENCE FRAME

To display corotation in the magnetic reference frame, the magnetic points desired for plotting are converted to geographic coordinates, then the corotation potentials are found in the geographic reference frame.

Figure 12, depicts the UT motion of the corotation pattern in the magnetic reference frame. Just as the center of the polar convection pattern moved in an 11° circle about the geographic pole, the corotation pattern moves in an 11° circle around the magnetic axis. At 0000 UT, the center of the corotation pattern is at approximately 0730 LT, due to the offset of the geomagnetic and geographic poles.

Adding polar convection yields the total patterns shown in Figure 13. In the magnetic reference frame, polar convection clearly dominates higher latitudes and corotation has its greatest affect at lower latitudes (Kelley, 1989). The region of interaction is the most dynamic and least understood portion of the plasma flow.

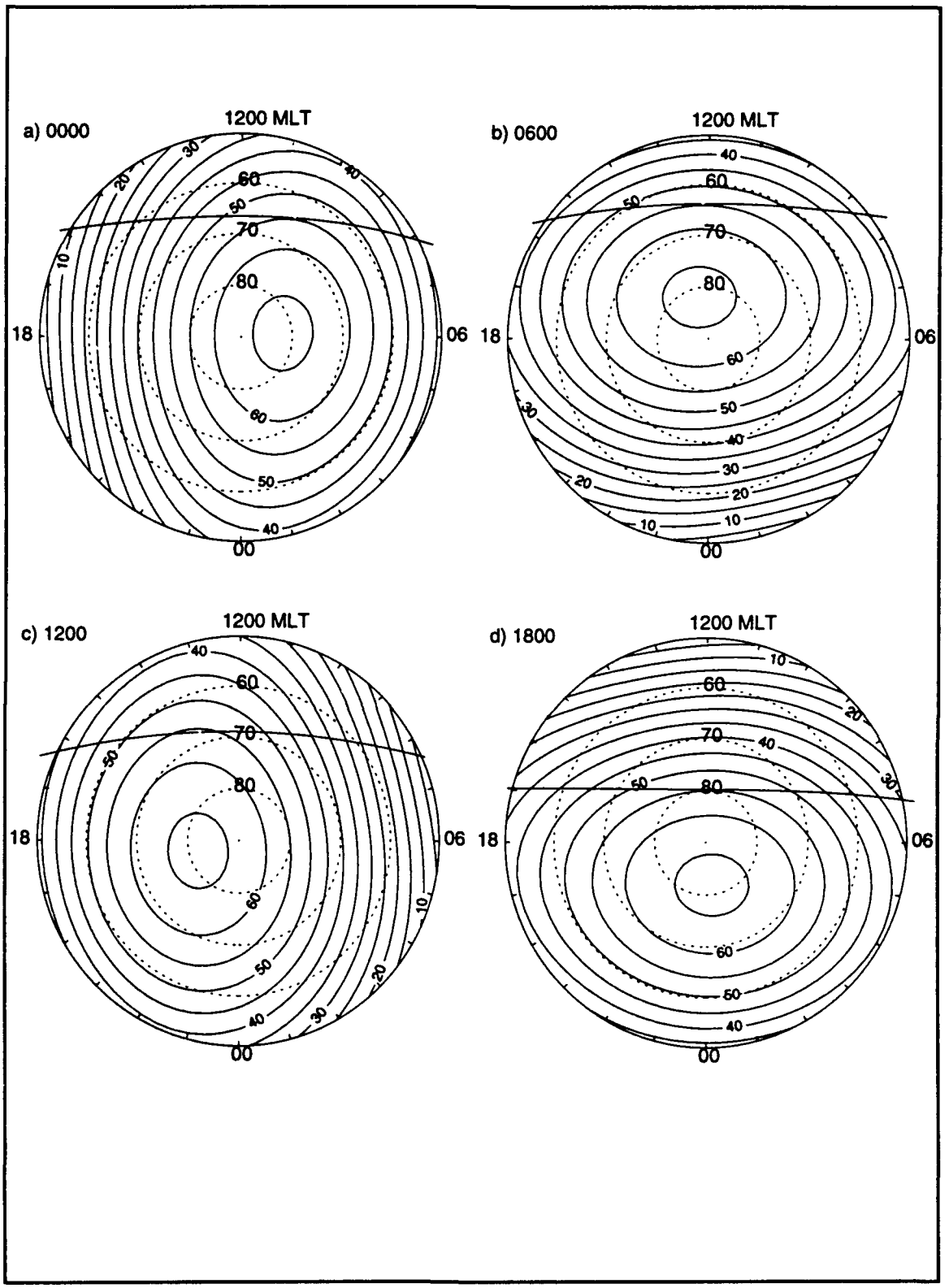

Figure 12. Corotation in the magnetic reference frame. Potentials are in kV. The solid line in the noon sector is the terminator on the ground.

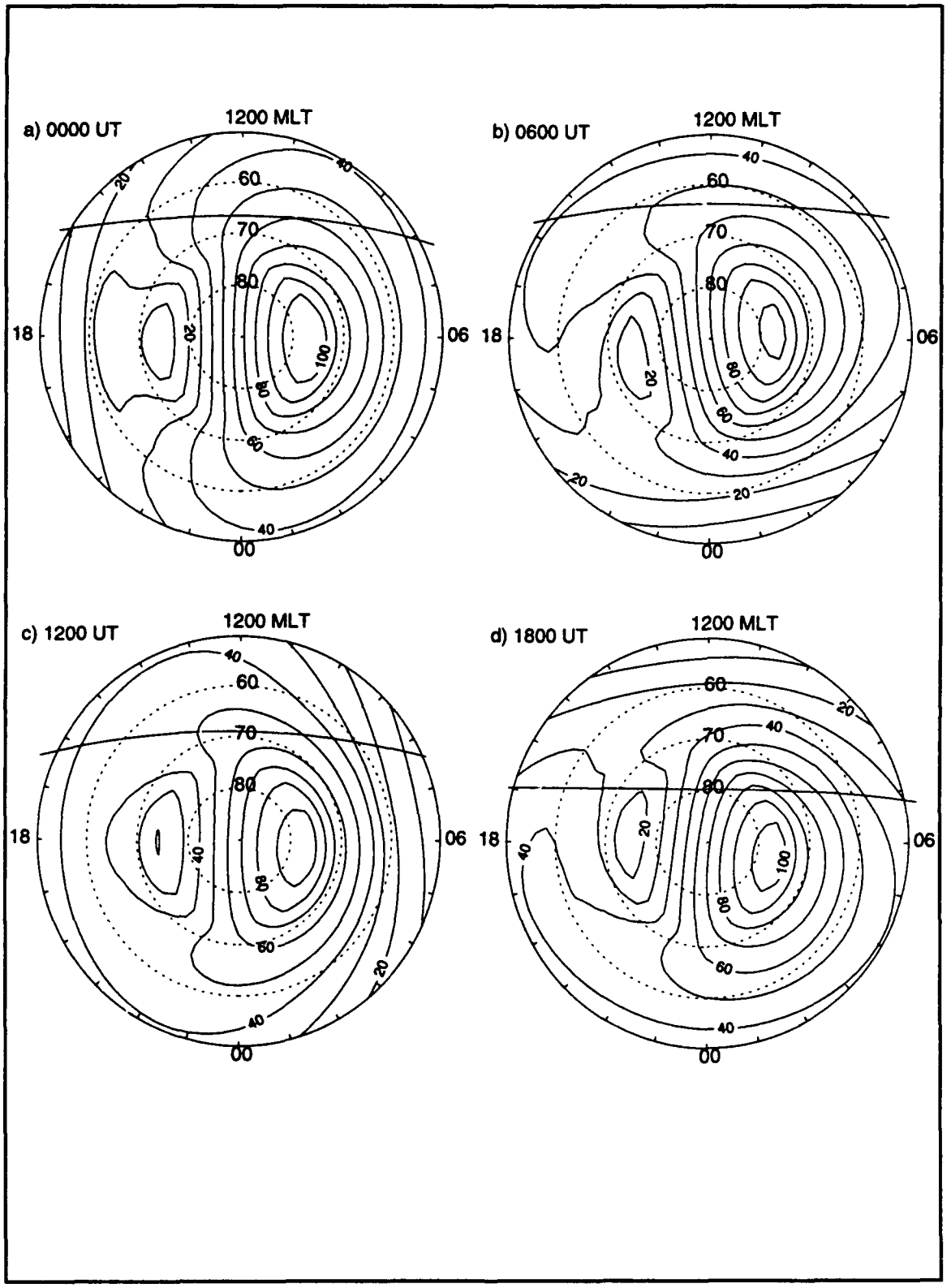

Figure 13. Total convection pattern in the magnetic reference frame. Potentials are in kV. The solid line in the noon sector is the terminator on the ground.

V. PLASMA TRAJECTORIES

With an understanding of the convection patterns and the reference frames in which they are displayed, the calculations of the plasma trajectories become fairly straightforward. The trajectory of a single plasma parcel will be discussed first, then extended to the motion of an entire region of plasma (a hole or patch). To calculate any trajectory, a velocity is required. Therefore, our first step is to calculate velocities from the equipotential patterns.

A. CALCULATING VELOCITY

The process for calculating the velocity from the equipotential patterns involves numerically differentiating the potentials to get an electric field, then using Equation (2.1) to find the velocity. Expressing Equation (2.3) in a slightly different way, the electric field in a given direction s is derived from the potential function

$$E_s = -\frac{\partial \Phi}{\partial s} \tag{5.1}$$

The potentials are stored in arrays that represent an even grid of latitudes and longitudes. Each row of the array corresponds to a specific latitude and each column corresponds to a specific longitude. The longitude ranges from 0° to 355° in 5° steps. The latitudes range from 50° latitude to 90° latitude in 2° steps. With the potential array arranged this way, the electric field component in the direction of lines of latitude are found by numerically differentiating the rows of the potential array. Similarly, the electric field components along lines of longitude are found by numerically differentiating the columns of the potential array.

The components used to express the velocities, electric field, and magnetic field are defined as x positive in the north direction, y positive in the east direction, and z positive in the vertically downward direction. Using the above method to calculate the electric field components, the z component of the electric field is not found. We are only considering motion along the surface of the sphere representing the ionosphere at 250 km

altitude in this thesis. Therefore it is acceptable to neglect the z component of the electric field.

With the electric field known, the magnetic field is required before we can use Equation (2.1). Fortran routines were available from JHU/APL that provide International Geomagnetic Reference Field (IGRF) components for a given date. Using those routines, magnetic field components were placed in arrays with the same structure as the potential and electric field arrays. Once the electric and magnetic fields were stored in similar arrays, algorithms were available in IDL that calculate cross products. Thus, Equation (2.1) could be used to find the velocity. The velocities were placed in arrays with the same structure as above. If the velocity was needed for a position that did not correspond to a specific position in the array, the array was interpolated using an algorithm available in IDL.

B. CALCULATING TRAJECTORIES

Calculating the plasma trajectories is straightforward. Starting at a known position, a velocity vector for that position is found from the velocity array already calculated. A distance and direction are then found by multiplying the velocity vector by a given time step. This distance and direction are added to the initial position using spherical trigonometry to find a new position. At the new position, a new velocity vector is found and the process is repeated.

All of these calculations are done in a rotating geographic reference frame, in geographic latitude and longitude. As discussed in Chapter II, corotation has no affect in this reference frame. It was also mentioned earlier that the magnetic coordinates were derived from mapping the magnetic field lines and therefore the lines of magnetic latitude are not evenly spaced. Hence, trajectory calculations are not easily calculated in the magnetic reference frame. Instead, they are calculated in the geographic frame and converted to the magnetic frame. The plasma trajectories are simply a series of geographic latitudes and longitudes with each point corresponding to a specific time.

Because the convection pattern changes with time as shown in Chapter IV, a new convection pattern and resulting velocities should be used for each step in the trajectory calculations. To balance accuracy and timely calculations, new convection patterns and resulting velocities are found every five minutes when Heelis' model is used and every ten minutes when the AMIE potentials are used.

When the calculated trajectories are plotted in the geographic inertial frame, the longitudes are converted to LT using Equation (3.1). To do this, the longitude is added to a time dependant angle. Thus, the conversion from longitude to LT accounts for corotation. Plasma trajectories are calculated using only the polar convection patterns in a rotating geographic reference frame.

To calculate the trajectory of an entire region of plasma, the region is first described as a series of 16 points that make a circle. Then the trajectory of each point is calculated. The position and shape of the region at any given time is described by the position of the 16 points at that time. Trajectories of both single plasma parcels and regions of plasma are presented in Chapter VI.

VI. RESULTS

The desired outputs for the model developed in this thesis were total equipotential patterns and plasma trajectories displayed in the geographic and geomagnetic inertial reference frames. The potential patterns will be presented first. Then trajectories of plasma parcels and areas of plasma will be presented.

A. POTENTIAL PATTERNS

Figures 11 and 13 depict the total convection patterns in the geographic and magnetic reference frames respectively. The solid line in the noon sector of the plots is the terminator on the ground. Plasma above the terminator would receive sunlight and plasma below the terminator would be in darkness. This is significant because plasma in sunlight would experience increased electron density due to solar ionization. Extended time in darkness can lead to depleted electron density, caused by chemical recombination and the formation of polar holes. Note that the terminator in Figure 11 does not move. It is considered stationary in the geographic frame for the 24 hours considered. In Figure 13, the terminator does move. Just as the corotation pattern moves in the magnetic reference frame, the terminator will move in the magnetic reference frame.

Referring to Figure 13, the strength of the electric fields and resulting velocities is proportional to the spacing between the lines of equipotential. The lines are spaced closer at the pole than at the lower latitudes in the dusk cell, implying a higher velocity across the pole. Likewise, the area near 2000 LT in Figure 13b is an area of stagnation, and potential electron density depletion. Another area that may lead to electron density depletion is the small dusk cell which may trap plasma in darkness. As convection patterns change in response to changes in the IMF, regions of stagnation and increased velocity will also change. A theory under study by Dr. Crowley involves a hole formed due to stagnation moving quickly to the dawn sector due to varying convection patterns.

Because varying convection patterns are central to Dr. Crowley's study, we have included the ability to use varying patterns in our model. Figure 14 depicts a pattern where the polar convection changes. The changes due to the IMF are most noticeable in

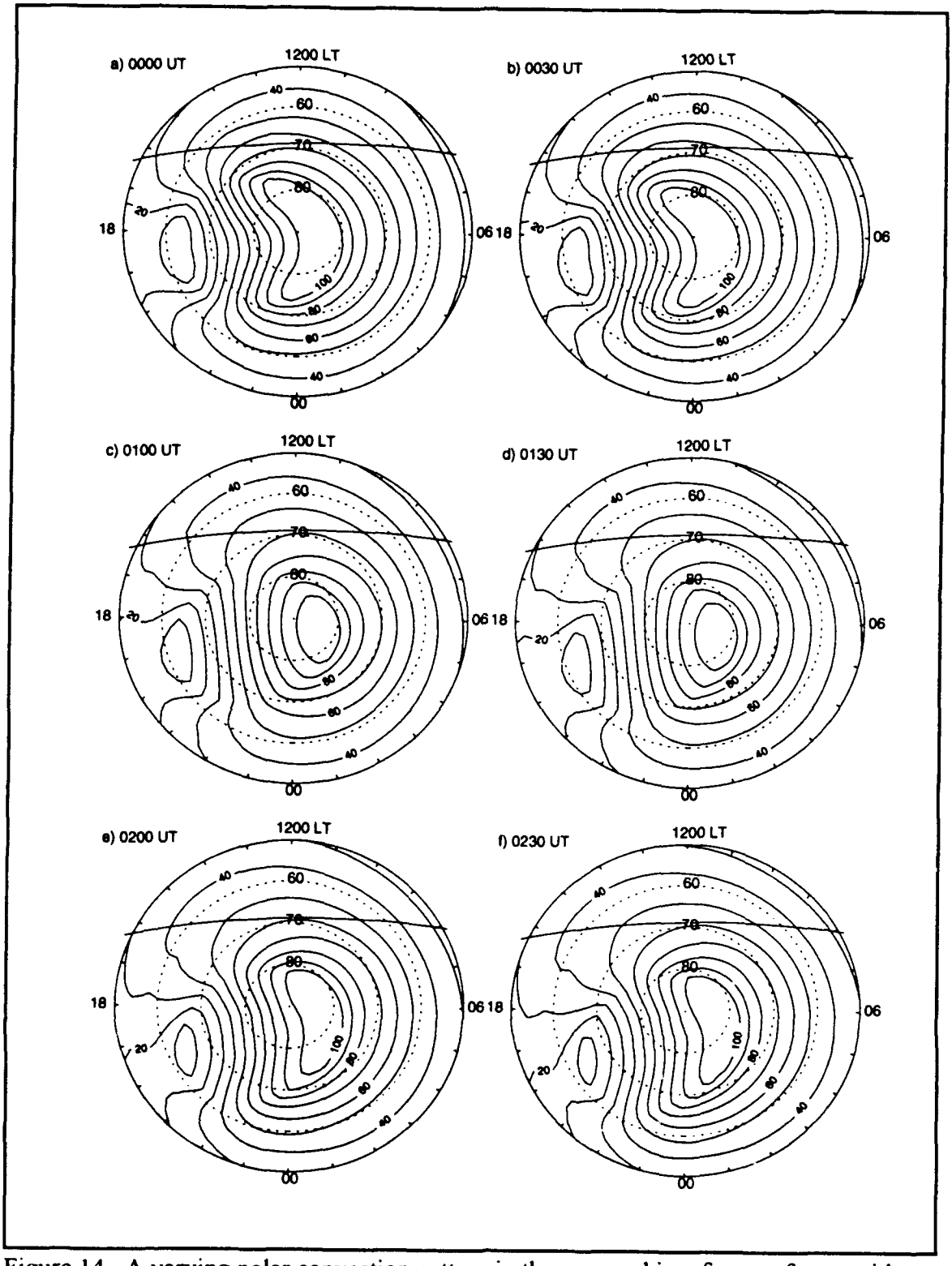

Figure 14. A varying polar convection pattern in the geographic reference frame with corotation accounted for. The IMF B_y component changes at 0100 UT and 0200 UT. The solid line in the noon sector is the terminator on the ground. Potentials are in kV.

the region of anti-sunward flow. Any polar convection pattern that can be created with Heelis' model can be used at any specified time with the algorithms we have developed.

Of particular interest to Dr. Crowley are the AMIE potentials for 16 January 1990. These are polar convection patterns that change every 10 minutes as the actual pattern for 16 January 1990 changed. With the AMIE potentials, the morphology of the polar hole detected by the DMSP F8 and DMSP F9 satellites on 16 Jan 1990 can be studied in greater detail. Figure 15 depicts the total equipotential patterns using the AMIE polar convection equipotentials at various times. These patterns are presented here as an example of the output of the algorithms developed.

A useful capability in IDL that can not be displayed in this thesis is the animation of the equipotential patterns. Images of the equipotentials are stored at desired time intervals and can be displayed in sequence. The speed at which they are displayed can be adjusted while the animation is being run. This is a very useful tool for visualizing the changes in the equipotentials that drive the plasma trajectories.

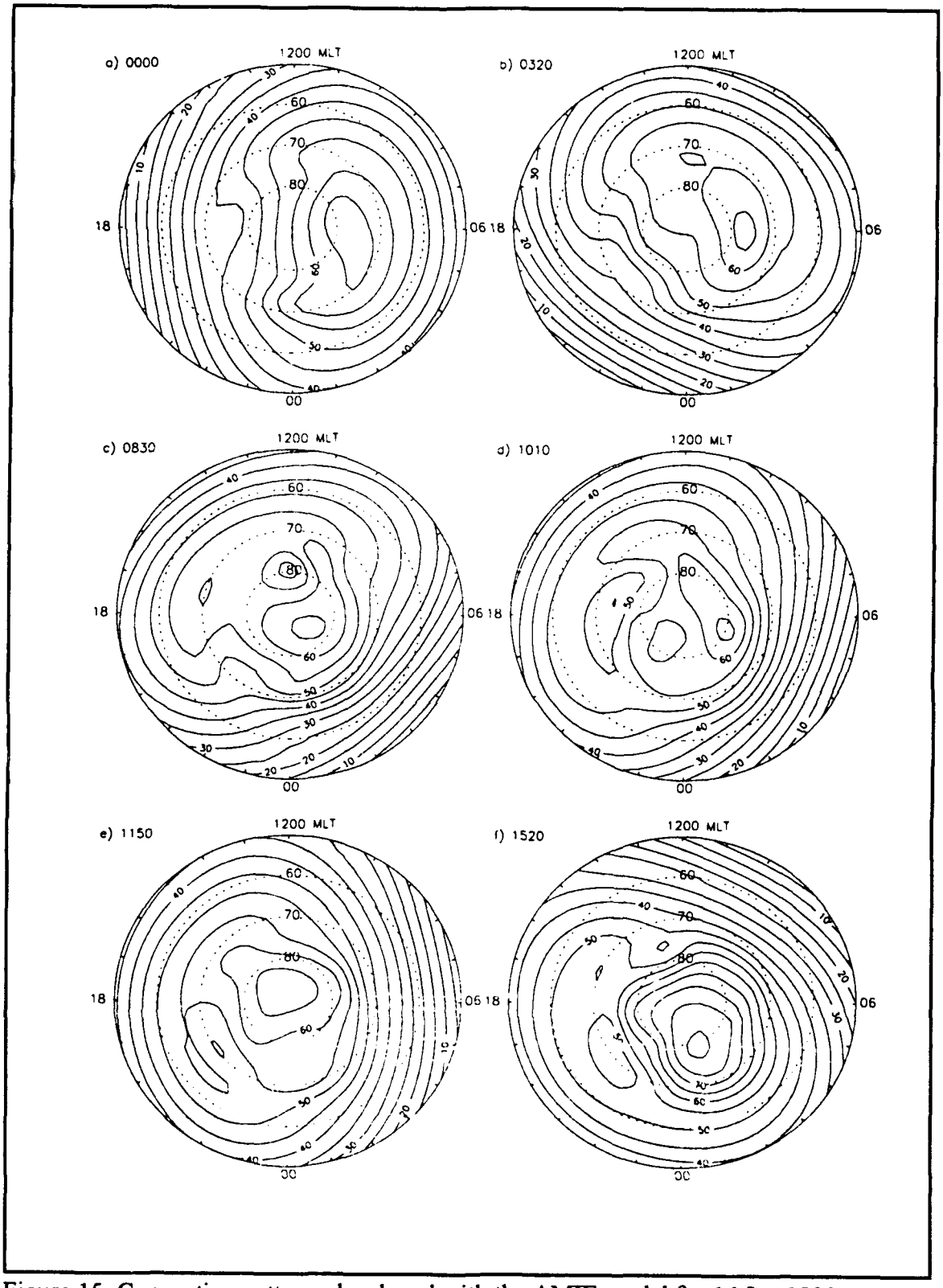

Figure 15 Convection patterns developed with the AMIE model for 16 Jan 1990. Corotation is added to the AMIE outputs. Equipotential patterns are in kV.

B. PARCEL TRAJECTORIES

There are an infinite number of possibilities for plasma trajectory start time, start positions and polar convection patterns. The simple algorithms developed in this thesis provide a tool for experimenting, quickly and easily, with conditions that affect plasma trajectories. Figures 16 through 18 will be used to illustrate one example of how the plasma trajectory may change unpredictably during 12 hours of universal time due to changes in start time or IMF orientation. The plasma trajectory is displayed in the geographic and magnetic reference frames (top left and bottom left of each figure respectively), and the last equipotential used in the trajectory calculations is displayed in both reference frames (top right and bottom right of each figure). The equipotential animation must be run separately, if desired.

The starting position for Figures 16 through 18 is 75° geographic latitude and 1800 LT. In Figure 16, the trajectory is started at 0000 UT. The solid line with diamonds represents the calculated trajectory. The diamonds are spaced at 30 minute intervals. This trajectory covers a large distance over 12 hours, moving around the dawn cell 1½ times. In Figure 17 the plasma parcel is again started in the same position but 6 hours later at 0600 UT. This time, the plasma parcel remains in the dusk cell, stagnating near 1800 LT. All of the starting conditions are the same for Figure 18 as for Figure 17, but the IMF orientation changes at 0900 UT and 1200 UT. There is no stagnation this time and the plasma parcel eventually becomes influenced by the dawn cell.

It would be difficult at best to predict these results by studying static figures of equipotentials. Even viewing the equipotential animation by itself would provide little help in predicting these parcel trajectories. Clearly, the combination of equipotential animation and trajectory calculation provides an invaluable tool for studying plasma motion.

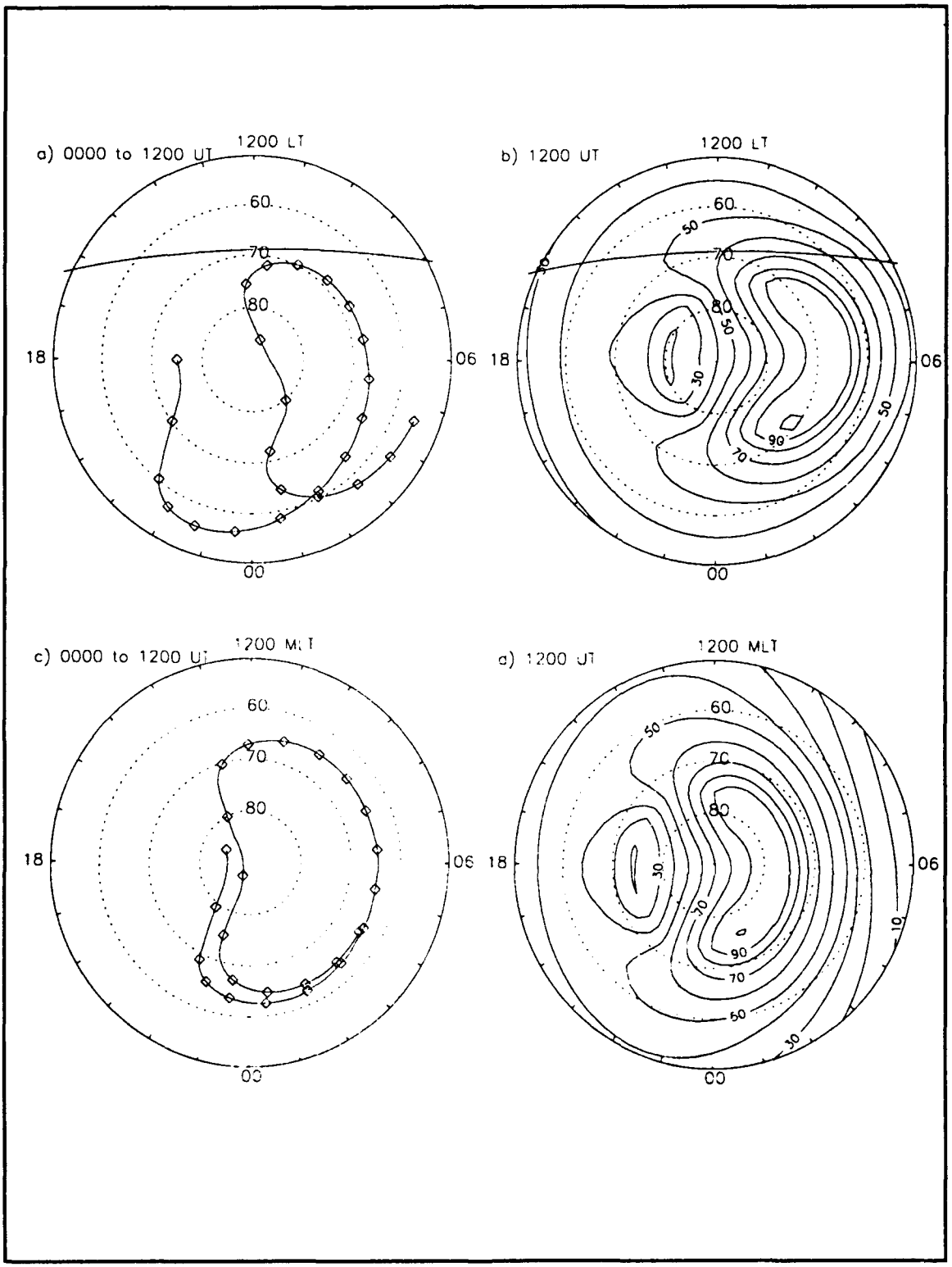

Figure 16. Plasma trajectory calculation output. Trajectory is started at 75° geographic latitude and 1800 LT. The trajectory was calculated from 0000 UT to 1200 UT. Spacing between diamond represents 30 minutes.

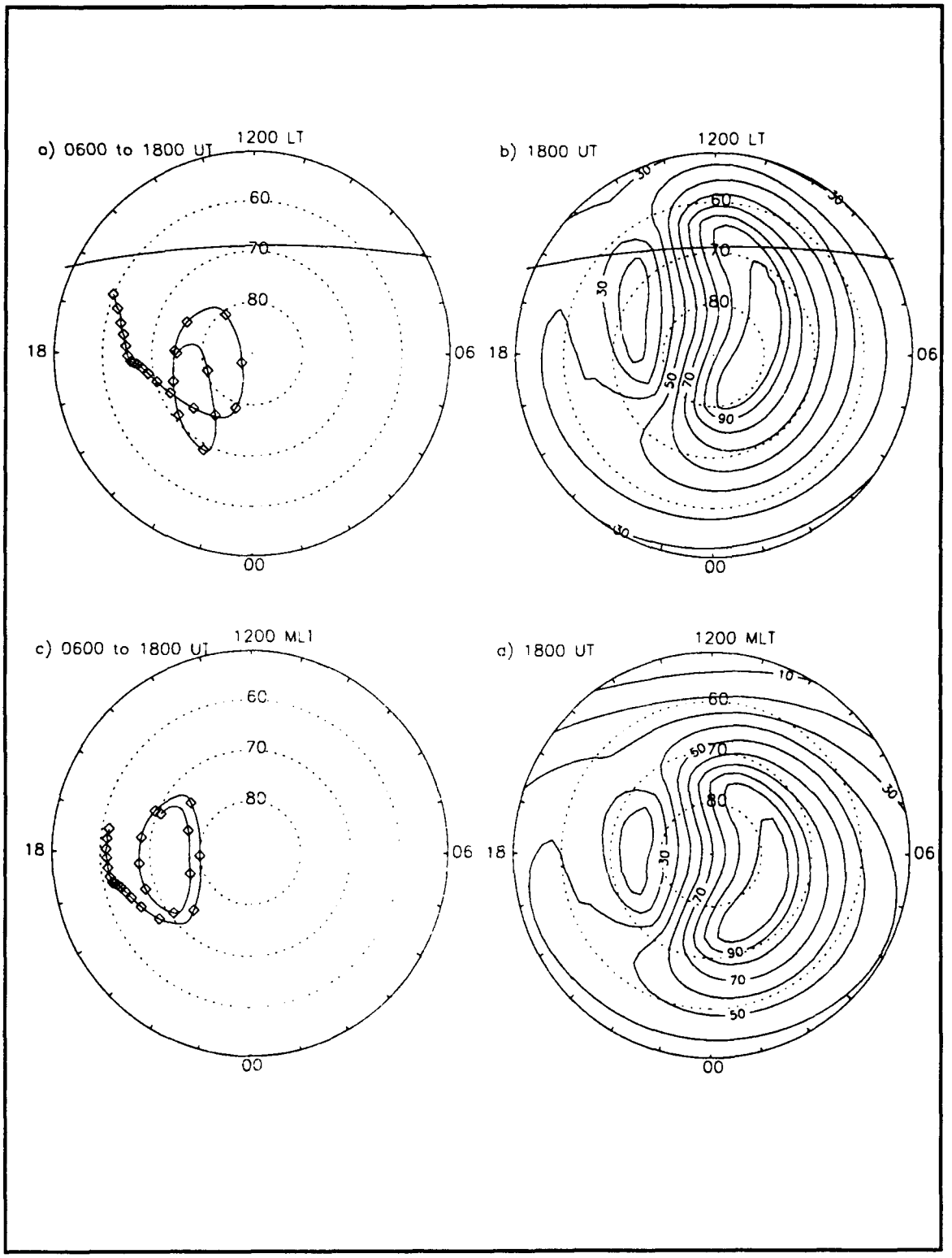

Figure 17. Plasma trajectory calculation output. Trajectory is started at 75° geographic latitude and 1800 LT. The trajectory was calculated from 0600 UT to 1800 UT. Spacing between diamond represents 30 minutes.

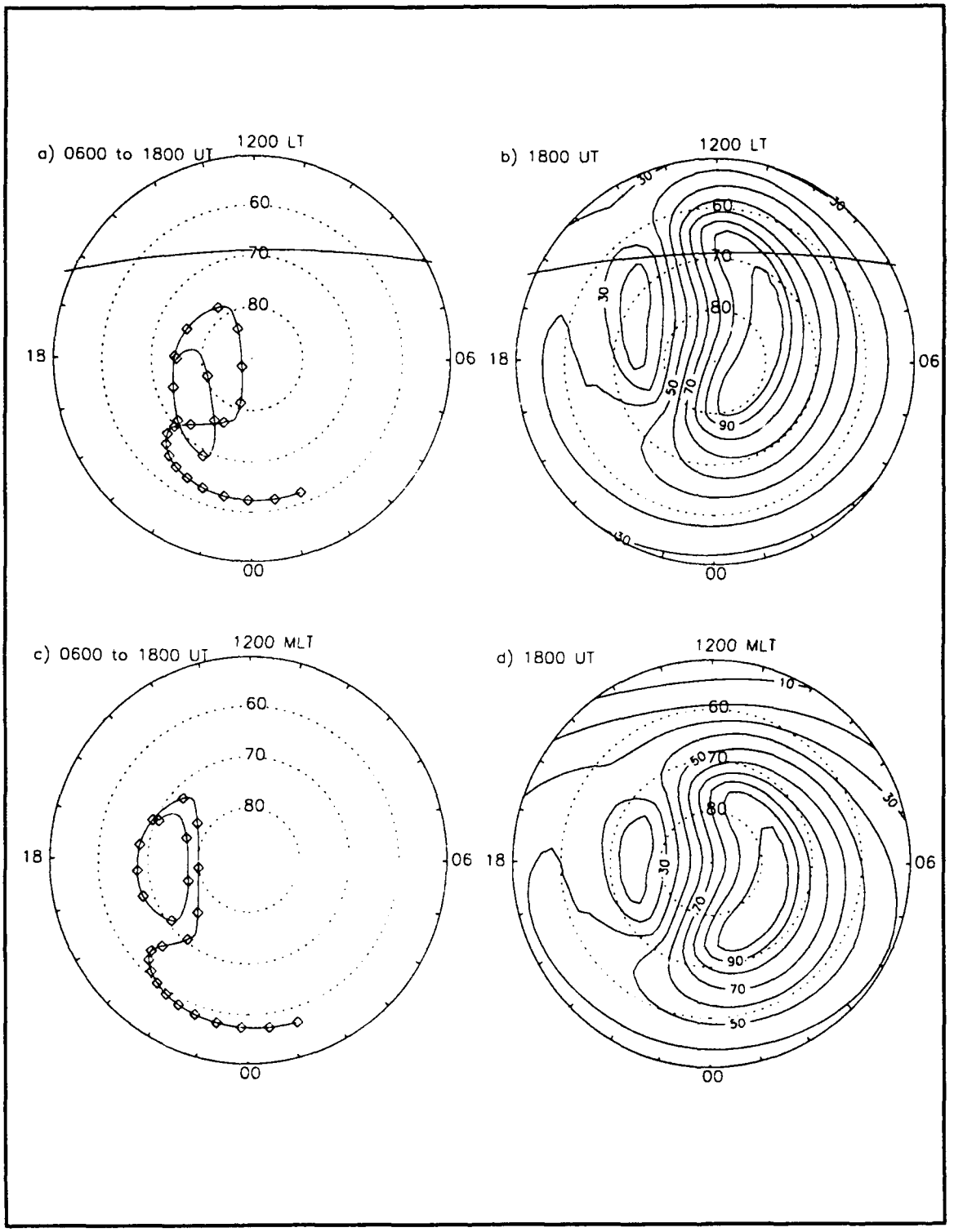

Figure 18. Plasma trajectory calculation output. Trajectory is started at 75° geographic latitude and 1800 LT. The trajectory was calculated from 0600 UT to 1800 UT. Spacing between diamond represents 30 minutes. IMF orientation changes from at 0900 UT and 1200 UT.

C. HOLE TRAJECTORIES

Figures 19 through 21 are outputs of trajectory calculations for polar holes. The polar holes are represented by circles at the beginning of the calculations. Since the trajectory calculations are not dependent on the electron density, the region inside the circle could represent an area of electron enhancement instead of a depletion. Because the motivation for developing this simulation was to study the polar hole of 16 January 1990 described by Crowley et al. (1993), the regions represented initially by a circle will be referred to as a hole.

Just as with the parcel trajectories, the hole may be started at any time and position. The center of the hole is placed at the given start position. The size of the hole may be adjusted as desired. For ease of comparison, the starting hole size is the same for Figures 19 through 21. Successive holes are plotted at 60 minute intervals. These figures are presented as examples of the outputs from the model developed in this thesis. No conclusions about the morphology of a hole can be made at this time.

A hole that moves quickly across the pole and reforms in the midnight sector is shown in Figure 19. Recently, Sojka et al. (1994) have used motion similar to that in Figure 19 to explain the formation of patches in the dark region of the polar ionosphere. Figure 20 depicts the motion of a hole under the combined affects of the dawn cell and corotation. The hole covers a considerable distance in 2 hours. Under the combined effects of the dusk cell and corotation, Figure 21 shows the stagnation of a hole over 2 hours. Although a portion of the hole moves to lower latitudes, the general position of the hole remains unchanged.

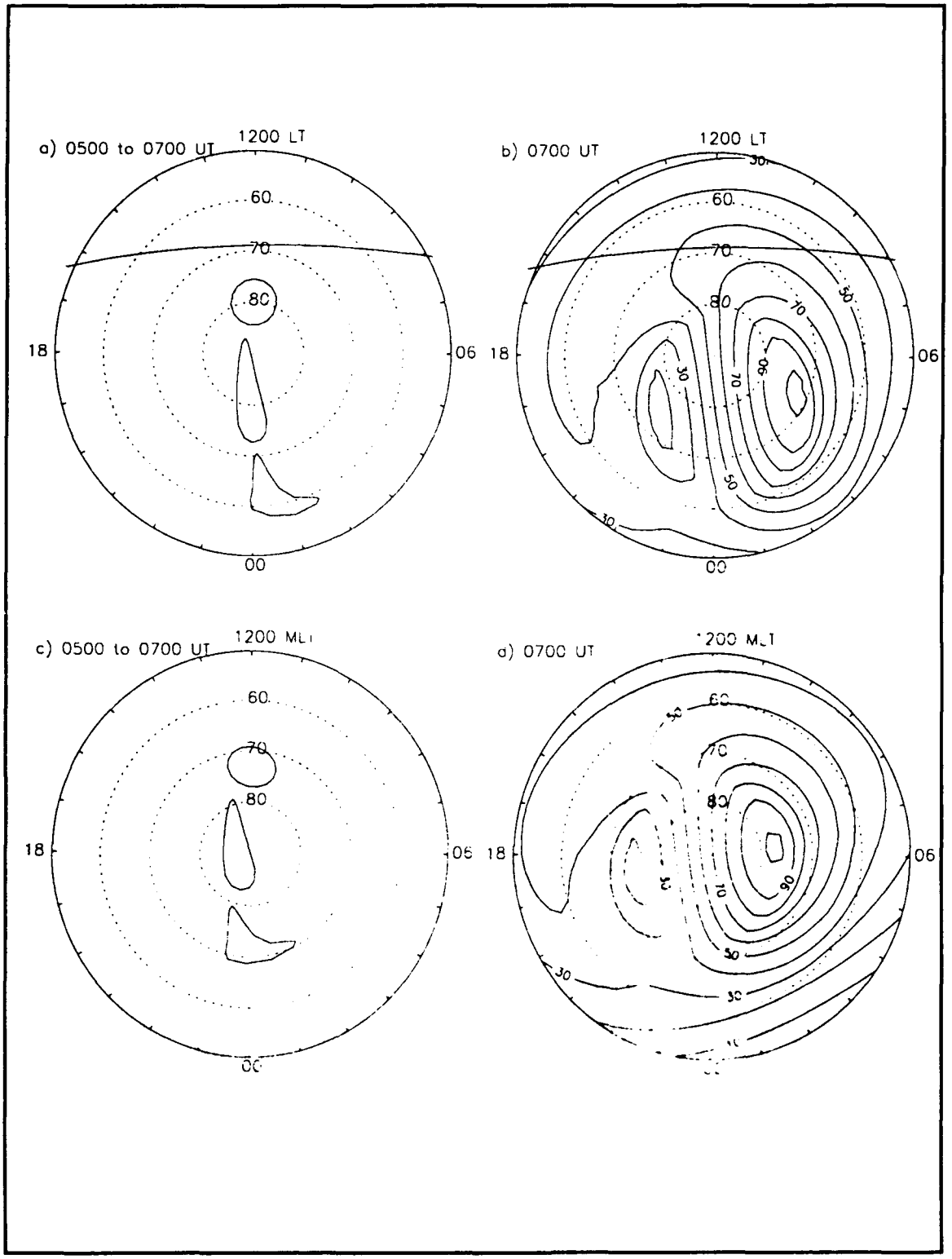

Figure 19. Trajectory of a polar hole started centered at 80° geographic latitude and 1200 LT. The trajectory was calculated from 0500 UT to 0700 UT. Successive holes are plotted at one hour intervals.

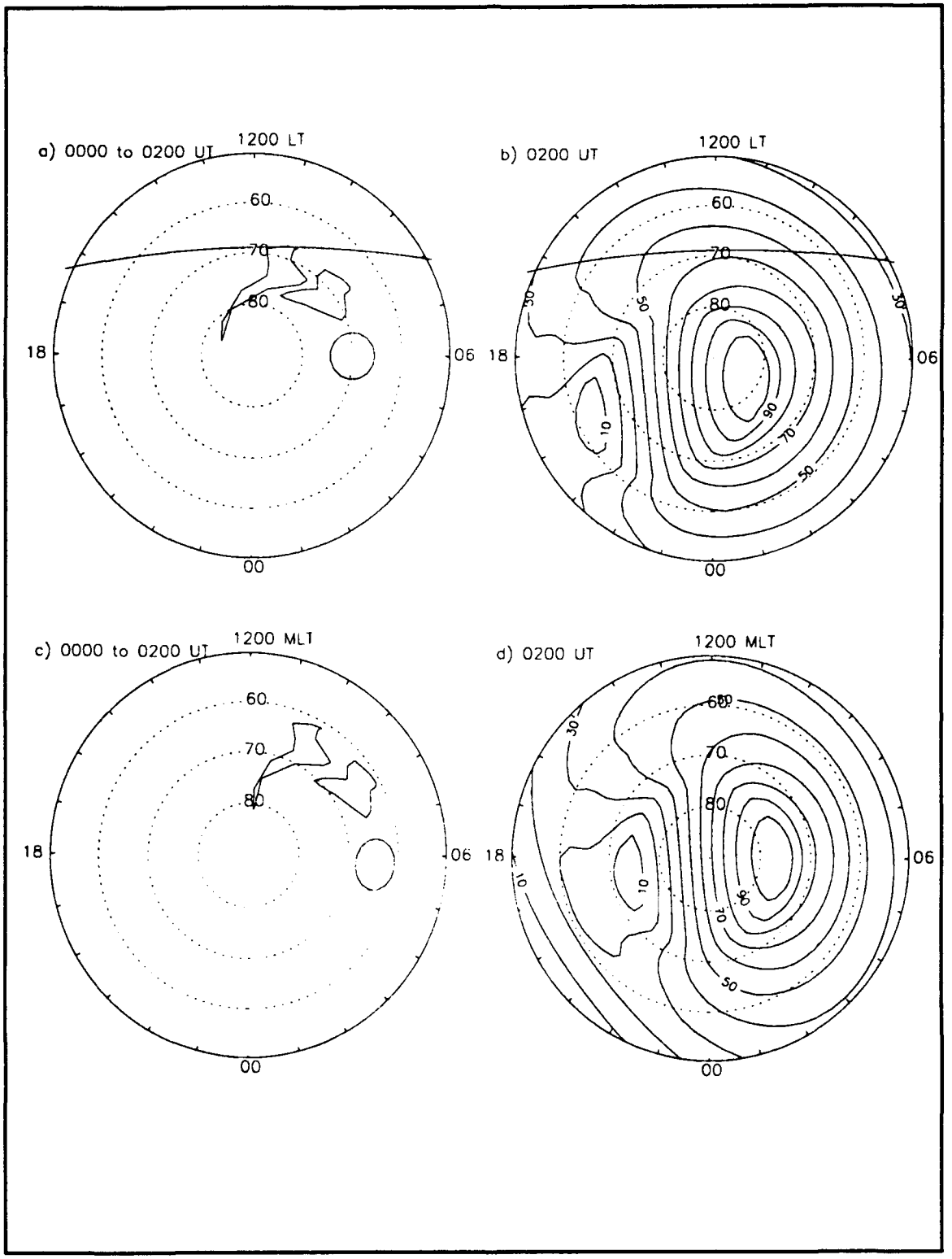

Figure 20. Trajectory of a polar hole started centered at 70° geographic latitude and 0600 LT. The trajectory was calculated from 0000 UT to 0200 UT. Successive holes are plotted at one hour intervals.

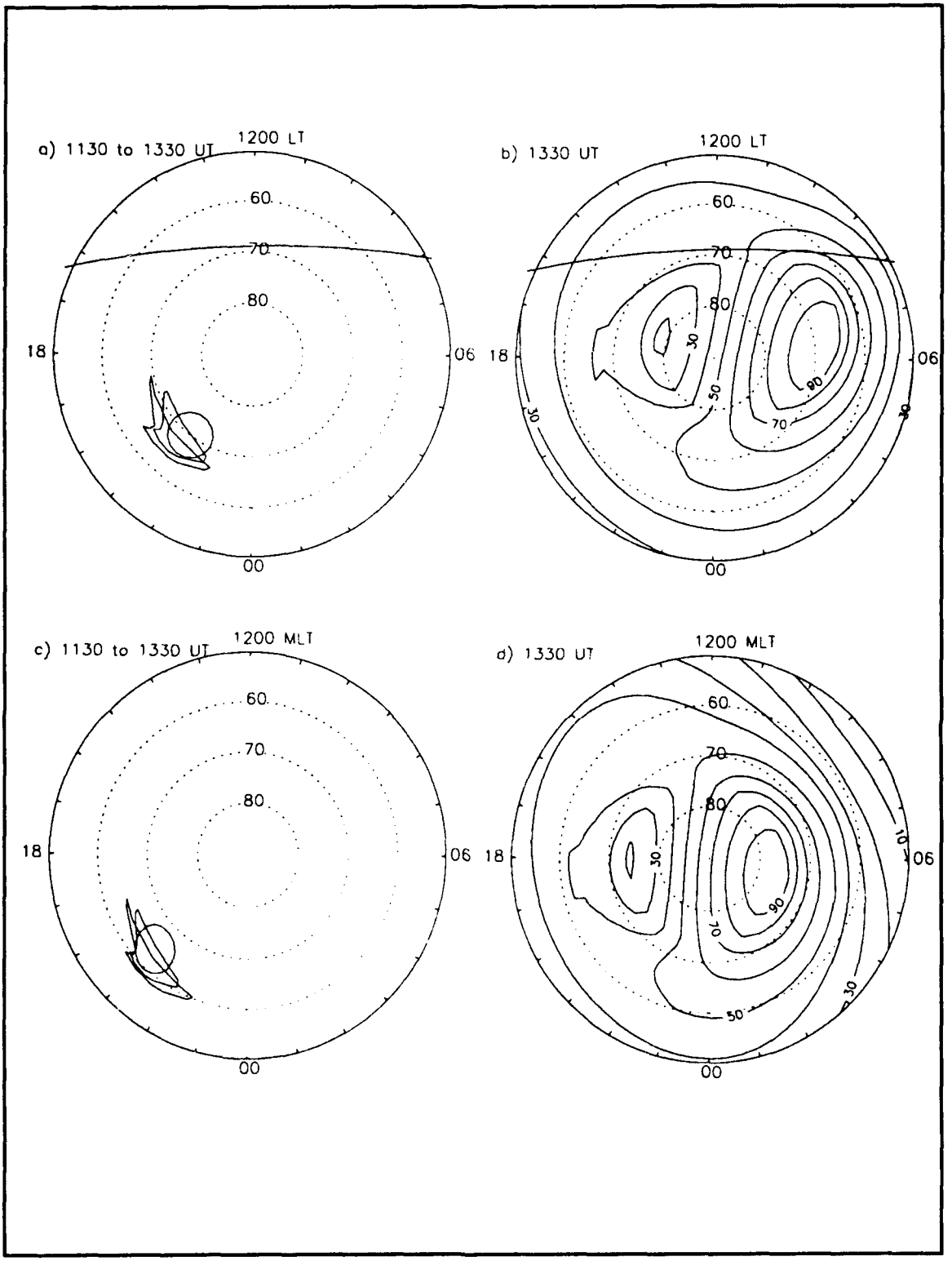

Figure 21. Trajectory of a polar hole started centered at 70° geographic latitude and 2100 LT. The trajectory was calculated from 1130 UT to 1330 UT. Successive holes are plotted at one hour intervals.

The actual location of the polar hole studied by Crowley et al. (1993) is depicted from 1010 UT to 1520 UT in Figure 22. The dashed lines are the satellite paths. The lines are solid where the polar hole was detected. The circle near the pole is the location of the ionosonde (Quanaq, Iceland). The circle is solid at times when the hole was detected. In this five hour period the polar hole moves from pre-midnight to post-midnight and appears to shrink in size significantly.

In Figure 23, motion of the hole is simulated using the AMIE potentials from 1010 UT to 1520 UT. The hole is started with the center at 77° geographic latitude and 2200 LT with a size representative of the actual hole at 1010 UT. At 1520 UT, the simulated hole has moved to basically the same position as the actual polar hole, although the simulated hole has become extremely distorted. As mentioned earlier, the polar hole is due stagnetion in darkness and solar illumination produces electrons that fill in the hole. The dashed line in Figure 23 is the 104° solar zenith angle (SZA) line projected on the surface of the earth. It was selected because it is considered the maximum SZA at which significant ionization occurs. Figure 23a reveals that, by 1520 UT, much of the initially depleted plasma has traversed the 104° SZA line into the day side. This would result in a filling in of the polar hole in those areas. The depleted plasma remaining on the night side of the 104° SZA line now represents a much smaller polar hole. This scenario reproduces the observed variation of the polar hole location and size in Figure 22. The above study illustrates the power of the model developed for this thesis. The results of a more detailed study will be published as a paper in the *Journal of Geophysical Research*.

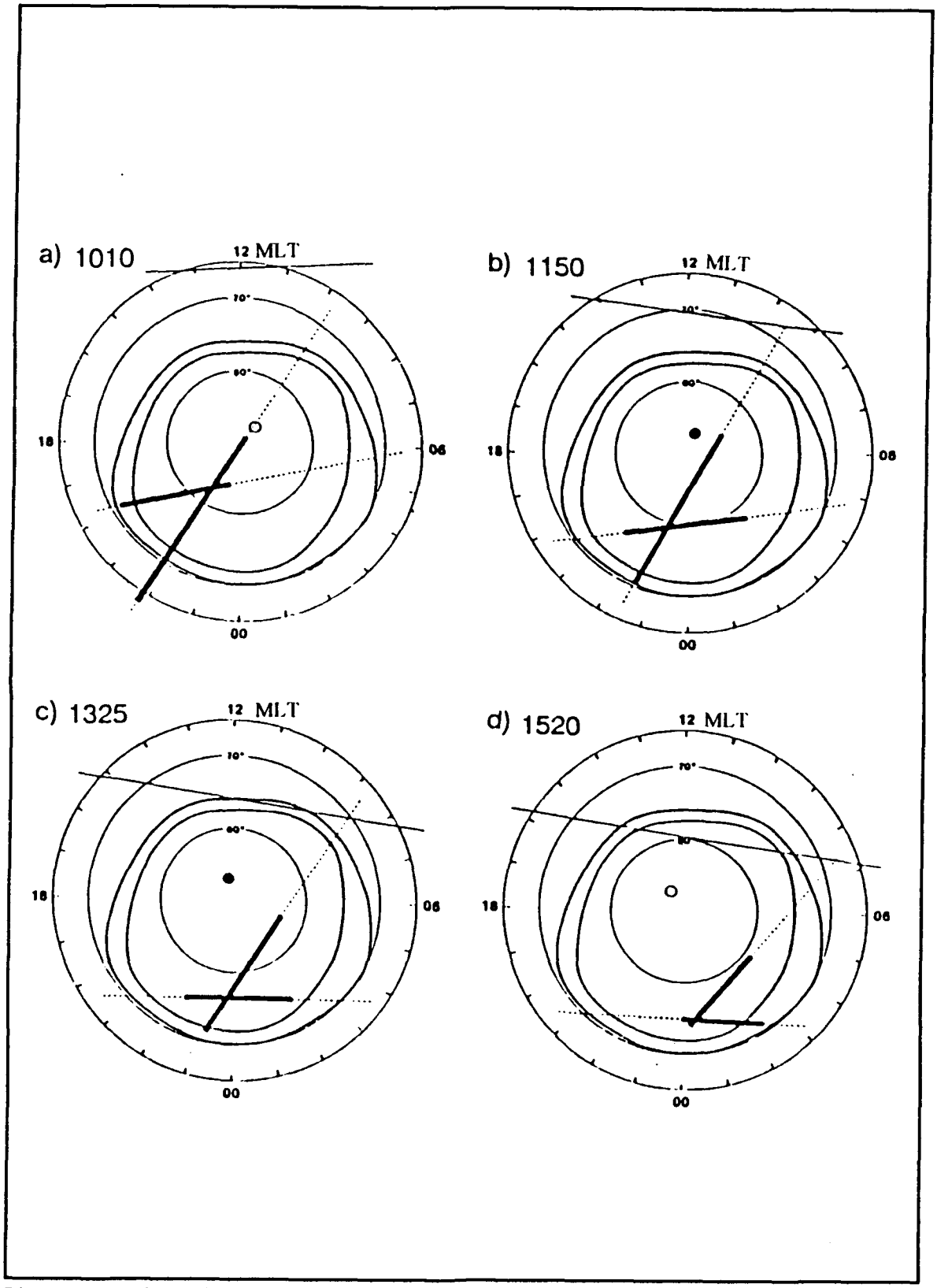

Figure 22. Polar hole location as detected by DMSP F8 and F9 on 16 January 1990.

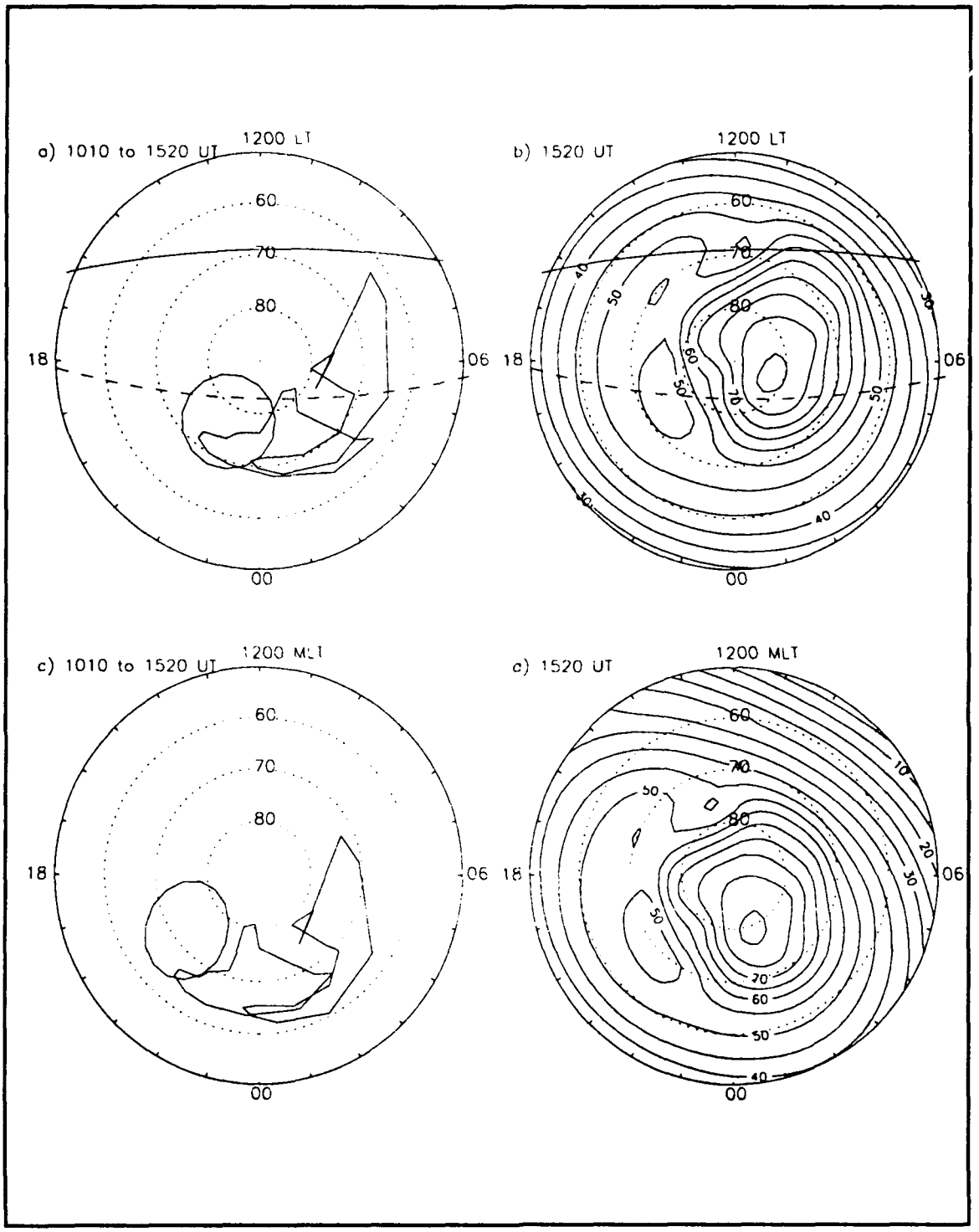

Figure 23. Trajectory of simulated polar hole using AMIE potentials for 1010 UT to 1520 UT, 16 January 1990. The hole was started with the center at 77° geographic latitude, 2200 LT. Successive holes are plotted in 155 minute intervals. The solid line in the noon sector is the terminator. The dashed line is the 104° solar zenith angle. Potentials are labeled in kV.

VII. CONCLUSIONS

Until recently, the majority of the work in the ionosphere at high latitudes has been theoretical, focusing on plasma motion in the magnetic reference frame. Recent studies have begun to examine satellite and ground based data expressed in the geographic reference frame. Understanding the relationships between the two reference frames as they move in time is difficult to visualize and predict. Further complicating the problem, the polar convection field changes in response to changes in the IMF.

The computer model that we developed can display the total convection patterns in both reference frames quickly and easily. Trajectories of both single plasma parcels and entire regions of plasma can be found for time lengths of up to 24 hours given any start time and position. Polar convection fields that are both steady or varying with time may be used, giving the model the flexibility to be compared with actual plasma motions detected by satellite and ground based systems. This provides an extremely useful tool for understanding the dynamic nature of high latitude plasma motion.

The usefulness of this tool was demonstrated by applying it to the study of polar hole motion observed on 16 January 1990 by the DMSP satellites. Qualitative changes in location and size of the hole were explained in terms of combining UT effects with changes in the IMF, which in turn resulted in changes in the convection pattern.

The model developed in this thesis is being used by scientists at JHU/APL to continue studying plasma motion on the polar regions. The effects of a changing IMF on polar plasma motion will be the topic of a paper under preparation by Dr. Crowley. As our understanding of plasma motion improves, so will our ability to predict the dynamic nature of the ionospheric communication windows in the polar regions. These communication windows are important in all areas of mission support in today's high technology warfare arena.

LIST OF REFERENCES

Baker, K. B., and Wing, S., "A New Magnetic Coordinate System for Conjugate Studies at High Latitudes", *Journal of Geophysical Research*, vol. 94, no. A7, pp. 9139-9143, 1 July 1989.

Brinton, H. C., Grebowsky, J. M., and Brace, L. H., "The High-Latitude Winter F Region at 300 km: Thermal Plasma Observations from AE-C", *Journal of Geophysical Research*, vol. 83, no. A10, pp. 4767-4776, 1 October 1978.

Crowley, G., Carlson, H. C., Basu, S., Denig, W. F., Buchau, J., and Reinisch, B. W., "The Dynamic Ionospheric Polar Hole", *Radio Science*, vol. 28, no. 3, pp. 401-413, May-June 1993.

Davis, L., Jr., "Stellar Electromagnetic Fields", *Physical Review*, vol. 72, no. 7, 1 October 1947.

Davis, L., Jr., "Stellar Electromagnetic Fields (Abstract)", *Physical Review*, vol. 72, p. 632, 1948.

Heelis, R. A., Lowell, J. K., and Spiro, R. W., "A Model of the High-Latitude Ionospheric Convection Pattern", *Journal of Geophysical Research*, vol. 87, no. A8, pp. 6339-6345, 1 August 1982.

Hones, E. W., Jr., and Bergeson, J. E., "Electric Field Generated by a Rotating Magnetized Sphere", *Journal of Geophysical Research*, vol. 70, no. 19, pp. 4951-4958, 1 October 1965.

Kelley, M. C., *The Earth's Ionosphere*, pp. 1-20, 24-62, 261-309, Academic Press, Inc., 1989.

Richmond, A. D., Kamide, Y., "Mapping Electrodynamic Features of the High-Latitude Ionosphere From Localized Observations: Technique", *Journal of Geophysical Research*, vol. 93, no. A6, pp. 5741-5759, 1 June 1988.

Richmond, A. D., Kamide, Y., Ahn, B. H., Akasofu, S. I., Alcayde, D., Blanc, M., Beaujardiere, O. de la, Evans, D. S., Foster, J. C., Friis-Christensen, E., T. J. Fuller-Rowell, J. M. Holt, Knipp, D. Kroehl, H. W., Lepping, R. P., Pellinen, R. J., Senior, C., and Zaitev, A. N., "Mapping Electrodynamic Features of the High-Latitude Ionosphere From Localized Observations: Combined Incoherent-Scatter Radar and Magnetometer Measurements for January 18-19, 1984", *Journal of Geophysical Research*, vol. 93, no. A6, pp. 5760-5776, 1 June 1988.

Sojka, J. J., Bowline, M. D., and Schunk, R. W., "Patches in the Polar Ionosphere: UT and Seasonal Dependence", *Journal of Geophysical Research*, vol. 99, no. A8, pp. 14959-14970, 1 August 1994.

The Joint Chiefs of Staff Memorandum MJCS serial 154-86 to Under Secretary of Defense (Research and Engineering), Subject: Military Requirements for Defense Environmental Satellites, 1 August 1986.

INITIAL DISTRIBUTION LIST

1. Defense Technical Information Center 2
   Cameron Station
   Alexandria, Virginia 22304-6145

2. Library, Code 52 2
   Naval Postgraduate School
   Monterey, California 93943-5101

3. Prof. D. D. Cleary, Code PH/Cl 3
   Naval Postgraduate School
   Monterey, California 93943-5000

4. Prof. O. Biblarz, Code AA/Bi 1
   Naval Postgraduate School
   Monterey, California 93943-5106

5. Chairman 1
   Space Systems Academic Group, Code SP
   Naval Postgraduate School
   Monterey, California 93943-5101

6. Raz Smith, Code EC 1
   Naval Postgraduate School
   Monterey, California 93943-5000

7. Dr. Geoff Crowley 1
   Mail Stop 24E-123
   Applied Physics Laboratory
   Johns Hopkins Road
   Laurel, Maryland 20723

8. Capt. David Deist 1
   3840 Masters Drive
   Colorado Springs, Colorado 80907

9. MCCDC, Code C46 1
   1019 Elliot Road
   Quantico, Virginia 22134-5027